

THE UNIVERSITY OF MICHIGAN  
COLLEGE OF LITERATURE, SCIENCE, AND THE ARTS  
Department of Physics

Technical Report

ROTATIONAL ENERGIES OF ASYMMETRIC ODD-A NUCLEI AND NUCLEI WITH A AROUND 190

Karl T. Hecht  
The University of Michigan

G. R. Satchler  
Oak Ridge National Laboratory

ORA Project 03114

under contract with:

DEPARTMENT OF THE NAVY  
OFFICE OF NAVAL RESEARCH  
NAVY THEORETICAL PHYSICS  
CONTRACT NO. Nonr 1224(15)  
WASHINGTON, D.C.

administered by:

OFFICE OF RESEARCH ADMINISTRATION

ANN ARBOR

August 1961

ABSTRACT

The asymmetric rotator model of Davydov and Filippov has been extended to odd-A nuclei by coupling a single nucleon to an inert core of well stabilized asymmetric equilibrium shape. Rotational energies are calculated for states with spin  $I$  through numerical diagonalization of  $(I + \frac{1}{2}) \times (I + \frac{1}{2})$  rotational matrices which depend in a complicated way on the state of the odd nucleon. The state of the odd nucleon is described by single particle wave functions such as those calculated by Newton, generalizations for the asymmetric case of the wave functions computed by Nilsson for axially symmetric nuclei. The rotational energy spectrum for a particular particle excitation is in general very rich in number of levels and may consist of a complicated sequence of spin values. In many cases, however, particularly for small asymmetries, the rotational spectra may consist of several well separated or overlapping sequences of spin states which resemble the rotational bands of axially symmetric nuclei, especially insofar as  $K$  (which gives the projection of  $I$  on the body-fixed  $z$  axis) may be approximately a good quantum number for each sequence.

In an initial survey of odd-A nuclei around  $A$  of 190 no clearcut evidence has been found for the existence of nuclei with a well defined asymmetric equilibrium shape. Calculations for  $\text{Ir}^{191}$  and  $\text{Re}^{185}$  indicate only that it may be very difficult to distinguish between a symmetric and an asymmetric rotator model when the asymmetry is small. Calculations for  $\text{Pt}^{195}$  show

that, although the observed level scheme can be reproduced by asymmetric rotator theory, the observed electromagnetic transition probabilities are not in agreement with the predictions of the simple asymmetric rotator model.

## INTRODUCTION

Since Davydov and Filippov<sup>1</sup> first suggested the validity of the asymmetric rotator modification for the strong coupling limit of Bohr's collective model<sup>2</sup>, surveys have been made by several authors<sup>3</sup> which seem to indicate that the model, in which the nucleus is pictured to have a well stabilized axially asymmetric equilibrium shape, may successfully describe the properties of low-lying levels of even-even nuclei in many different regions of the periodic table. However, since the  $I = 2$  and  $3$  rotator levels, particularly in the limiting case of large asymmetry, have properties very similar to those predicted on the basis of the vibrational model, the validity of the asymmetric rotator model has been questioned by other authors who point out that many of the predictions of the Davydov-Filippov model are also in quantitative agreement with the vibrational model with appropriate refinements<sup>4</sup>. The calculations of Newton<sup>5</sup>, on the other hand, indicate that the axially symmetric equilibrium shape of the Nilsson model nucleus<sup>6</sup> is perhaps not always the intrinsically most stable. It was therefore thought worthwhile to extend the asymmetric rotator model to the case of odd-A nuclei. In order to afford a further possible test of

the model, however, the nuclei to be studied should have preferably both large asymmetry and, equally important, a well defined equilibrium shape, that is small vibration-rotation interactions. The work of Davydov<sup>7</sup> on even nuclei suggests that the sequence Os<sup>186</sup>, Os<sup>188</sup>, Os<sup>190</sup>, and Os<sup>192</sup> may satisfy both of these requirements better than nuclei in other regions of the periodic table. The theory will therefore be applied in particular to odd-A nuclei in the vicinity of  $A \sim 190$ .

#### THE MODEL

It will be assumed that a single nucleon is coupled to an inert core of asymmetric equilibrium shape. The rotational Hamiltonian<sup>2</sup> has the form

$$H_{\text{rot}} = \frac{\hbar^2}{2\mathcal{I}_x} (I_x - j_x)^2 + \frac{\hbar^2}{2\mathcal{I}_y} (I_y - j_y)^2 + \frac{\hbar^2}{2\mathcal{I}_z} (I_z - j_z)^2 \quad (1)$$

where the inertial parameters are such that  $\mathcal{I}_x \neq \mathcal{I}_y \neq \mathcal{I}_z$ . The operators  $I_k$  and  $j_k$  describe the body fixed components of the total angular momentum of the nucleus and the angular momentum of the odd nucleon, respectively. For the present it will be assumed that the wave function which describes the motion of the odd nucleon in the ellipsoidal potential field is known in the form

$$\chi_{\text{particle}} = \sum_{j\Omega} c_{j\Omega} \chi_{\Omega}^j \equiv \chi_{\nu} \quad (2)$$

where  $\chi_{\Omega}^j$  are eigenfunctions of  $j^2$  and  $j_z$ . In the limit of zero deformation (spherical shell model limit) all but one of the coefficients  $c_{j\Omega}$  are equal to zero in a particular state. In the limit of axial symmetry  $\Omega$  is a good quantum number, and the summation extends only over the possible values of  $j$ . In the asymmetric case ellipsoidal symmetry still imposes some restrictions. The Hamiltonian can depend on the angular coordinates of the odd nucleon, defined relative to the principal axis system of the ellipsoid, only through the spherical harmonics,  $Y_{00}^2$ ,  $Y_{20}^2$ , and  $Y_{-20}^2$ . As a result the summation over  $\Omega$  will involve either the values  $(+\frac{1}{2} \pm 2n)$  or  $(-\frac{1}{2} \pm 2n)$  with  $n = 0, 1, 2, \dots$ . The two types of coefficients are related by  $c_{j,-\Omega} = (-1)^{j-\frac{1}{2}} c_{j\Omega}$ . The complementary state  $\chi_{-\nu}$ , formed with  $\sum_{j\Omega} c_{j,-\Omega} \chi_{-\Omega}^j$ , is degenerate with  $\chi_{\nu}$ , as in the axially symmetric limit. In the strong coupling approximation the wave function of the system is made up of products of the particle wave functions and the rotational wave functions,  $D_{MK}^I$ . (The wave function which describes the zero point vibrational motion will be understood but not explicitly written.) The total wave function must have the specific symmetry<sup>2</sup>

$$\begin{aligned} \Psi &= \sum_K C_K \Psi_K = \sqrt{\frac{2I+1}{16\pi^2}} \sum_K C_K \sum_{j\Omega} c_{j\Omega} \left\{ D_{MK}^I \chi_{\Omega}^j + (-1)^{I-j} D_{M-K}^I \chi_{-\Omega}^j \right\} \\ &= \sqrt{\frac{2I+1}{16\pi^2}} \sum_K C_K \left\{ D_{MK}^I \chi_{\nu} + (-1)^{I-\frac{1}{2}} D_{M-K}^I \chi_{-\nu} \right\} \end{aligned} \quad (3)$$

where  $(K - \Omega)$  must be an even integer. This can be accomplished

by restricting the summation over both  $K$  and  $\Omega$  to the set of values

$$\dots, -\frac{11}{2}, -\frac{7}{2}, -\frac{3}{2}, \frac{1}{2}, \frac{5}{2}, \frac{9}{2}, \frac{13}{2}, \dots$$

This restriction is indicated by the prime on the summation symbols. The coefficients  $C_K$  which determine the  $K$ -admixture in a given rotational state are to be determined from the solution of the rotational problem, - unlike the coefficients  $c_{j\Omega}$  which are assumed known for each particular state of particle excitation. In the axially symmetric limit  $K$  is a good quantum and all but one of the coefficients,  $C_K$ , go to zero. Similarly only one  $\Omega$  remains, although there is still a sum over  $j$ . We then have  $K = \Omega$ , (the  $K \neq \Omega$  states are infinitely high in energy). The above convention for the values assumed by  $K$  and  $\Omega$  means that the wave function reduces to that of Bohr and Mottelson<sup>2,6</sup> for  $K = \Omega = (\frac{1}{2} + 2n)$  in the symmetric limit, but  $(-1)^{I-j}$  it for  $K = \Omega = (-\frac{1}{2} + 2n)$  where  $n$  is integral.

#### ROTATIONAL ENERGIES

It will be useful to introduce the rotational angular momentum operator  $\underline{R}$ , ( $\underline{R} = \underline{I} - j$ ). In terms of  $\underline{R}_i$ , the rotational Hamiltonian has the simple form

$$H_{rot} = \frac{\hbar^2}{2\mathcal{I}_x} R_x^2 + \frac{\hbar^2}{2\mathcal{I}_y} R_y^2 + \frac{\hbar^2}{2\mathcal{I}_z} R_z^2 \quad (4)$$

which will be particularly useful if a change is made from the  $|IKj\Omega\rangle$  representation of Eq. (3) to an  $|IjRK_R\rangle$  representation. ( $R$  and  $K_R$  are the quantum numbers which determine the magnitude and the body-fixed  $z$  component of the rotational angular momentum, respectively.)

$$\sqrt{\frac{2I+1}{8\pi^2}} D_{MK}^I \chi_{\Omega}^j = \sum_R (-1)^{j-\Omega} \langle IjK-\Omega | IjRK_R \rangle \psi_{K_R}^{IjR} \quad (5)$$

The unusual phase factor and the unusual sign in the Clebsch-Gordan coefficient arise from the fact that the angular momentum coupled wave function is constructed for the case of angular momentum subtraction rather than addition. ( $R = I - j$ ;  
 $K_R = K - \Omega$ ).\*

Davydov<sup>8</sup> has treated the special case of an odd- $A$  nucleus in which the intrinsic particle state is assumed to be such that  $j$  is a good quantum number and has the special value  $j = \frac{1}{2}$ . The  $|IjRK_R\rangle$  representation is particularly useful to show that the rotational energies in this very special case have exactly the same values as the rotational energies of even-even nuclei with corresponding values of  $R$ . Each rotational energy level, however, is doubly degenerate corresponding to the two possible values  $I = R \pm \frac{1}{2}$ . The total wave function, of symmetry given by Eq. (3), leads to a rotational wave function

\*A similar representation has been used by Osborn and Klema. Nuovo Cimento 9 (10), 791 (1958).

made up of terms of the form

$$\frac{1}{\sqrt{2}}(\Psi_{K_R}^{IjR} + (-1)^R \Psi_{-K_R}^{IjR}) \quad (K_R \text{ even}) \quad (6)$$

In the special case  $R = 3$ , for example, only one such linear combination exists, corresponding to  $|K_R| = 2$ . When the quantum numbers have the values  $R = 3$ ,  $|K_R| = 2$ ,  $j = \frac{1}{2}$ , the total spin  $I$  can have the two possible values  $5/2$  and  $7/2$ , so that two independent (orthogonal) wave functions can be constructed with  $R = 3$ . Application of Eq. (5) gives,

with  $I = 5/2$

$$\frac{1}{\sqrt{2}}(\Psi_{2}^{5/2, 1/2, 3} - \Psi_{-2}^{5/2, 1/2, 3}) = \left(\frac{6}{16\pi^2}\right)^{1/2} \left\{ \frac{1}{\sqrt{6}}(D_{M^{5/2}}^{5/2} \chi_{1/2}^{1/2} + D_{M^{-5/2}}^{5/2} \chi_{-1/2}^{1/2}) - \sqrt{\frac{5}{6}}(D_{M^{-3/2}}^{5/2} \chi_{1/2}^{1/2} + D_{M^{3/2}}^{5/2} \chi_{-1/2}^{1/2}) \right\}$$

and with  $I = 7/2$

$$\frac{1}{\sqrt{2}}(\Psi_{2}^{7/2, 1/2, 3} - \Psi_{-2}^{7/2, 1/2, 3}) = \left(\frac{8}{16\pi^2}\right)^{1/2} \left\{ \frac{\sqrt{3}}{2}(D_{M^{5/2}}^{7/2} \chi_{1/2}^{1/2} - D_{M^{-5/2}}^{7/2} \chi_{-1/2}^{1/2}) - \frac{1}{2}(D_{M^{-3/2}}^{7/2} \chi_{1/2}^{1/2} - D_{M^{3/2}}^{7/2} \chi_{-1/2}^{1/2}) \right\}$$

Since both of these wave functions result in exactly the same linear combination of  $R$  and  $K_R$  values, and since the matrix elements of the rotational Hamiltonian can be functions of the quantum numbers  $R$  and  $K_R$  only, (as can be seen from Eq. (4)), both of these states have the same rotational energy. Also, since the rotational Hamiltonian operates on an eigenfunction of  $R$  in exactly the same way in which the rotational Hamiltonian for an even-even nucleus operates on an eigenfunction of  $I$ , this energy has the same value as the rotational energy of an even-even nucleus with  $I = 3$ . Al-



together there are three independent wave functions with  $I = 5/2$  and four with  $I = 7/2$ , corresponding to the possible number of values of  $|K|$ . The two  $I = 5/2$  states orthogonal to the  $R = 3$  state above have asymmetric rotator wave functions with  $R = 2$  and energies which are identical with those of the two possible  $I = 3/2$  states. The complete energy spectrum consists of a non-degenerate  $I = \frac{1}{2}$  ( $R = 0$ ) ground state, the two different doubly degenerate  $I = 3/2, 5/2$  ( $R = 2$ ) states, the single doubly degenerate  $I = 5/2, 7/2$  ( $R = 3$ ) state, three different doubly degenerate  $I = 7/2, 9/2$  ( $R = 4$ ) states, and so forth, all with the same energies as the analogous rotational states in even-even nuclei.<sup>1</sup> If the particle wave function is only approximately a pure  $j = \frac{1}{2}$  function, the degeneracies are removed and the rotational energy spectrum should consist of doublets with  $I = R \pm \frac{1}{2}$ . Since no example is known for which  $j = \frac{1}{2}$  is even a moderately good approximation this very special case is of academic interest only. However, it does illustrate a general feature. The rotational energy spectrum of an asymmetric odd-A nucleus may be very rich in total number of levels compared with an axially symmetric nucleus.

In the strong coupling approximation the particle wave function in a given state is well specified independently of the rotational state of the nucleus. In an odd-A asymmetric nucleus a realistic particle wave function in general involves many different values of  $j$  and  $\Omega$ , so that products of the form,  $(\sum_{j\Omega} c_{j\Omega} \chi_{\Omega}^j) D_{MK}^I$ , lead to rotational wave functions which

are linear combinations of many different values of R. Since R is no longer a good quantum number, there will be no simple correlation between the rotational states of odd and even-even nuclei, and the rotational energies will depend in a complicated way on the state of the odd nucleon. Either the  $|IKj\Omega\rangle$  or the  $|IjRK_R\rangle$  representation can be used to compute the matrix elements of the rotational Hamiltonian. For given I (and specified particle excitation) there will be  $(I + \frac{1}{2})$  independent wave functions corresponding to the  $(I + \frac{1}{2})$  possible values of  $|K|$ , so that the determination of the rotational energies with spin I will involve the diagonalization of  $(I + \frac{1}{2}) \times (I + \frac{1}{2})$  matrices, (provided the strong coupling limit applies; that is, provided the rotational energies are small compared with the single particle excitations so that matrix elements of the rotational Hamiltonian between different particle states can be neglected). In terms of the rotational constants

$$A_1 = \hbar^2/2\mathcal{J}_x, \quad A_2 = \hbar^2/2\mathcal{J}_y, \quad A_3 = \hbar^2/2\mathcal{J}_z \quad (7)$$

the rotational energy for the state  $I = \frac{1}{2}$ , ( $K = \frac{1}{2}$ ) is given by

$$I = \frac{1}{2}: \quad E_{\text{rot}} = -\frac{1}{2}(A_1 + A_2)(a+b) - \frac{1}{2}(A_1 - A_2)c + A_3 \langle K_R^2 \rangle \\ + (A_1 + A_2)d + (A_1 - A_2)e \quad (8)$$

where the parameters a, b, c, d, and e, and  $\langle K_R^2 \rangle$  are determined by the state of the odd nucleon. The parameter a is the decoupling parameter familiar from the theory of axially symmetric nuclei

$$a = \sum_j c_{j\frac{1}{2}}^2 (-1)^{j-\frac{1}{2}} (j+\frac{1}{2}) \quad (9)$$

In the asymmetric case it is replaced by

$$(a+b) = \sum'_{j\Omega} c_{j\Omega} c_{j-(\Omega-1)} (-1)^{j-\frac{1}{2}} [(j+\Omega)(j-\Omega+1)]^{\frac{1}{2}} \quad (10)$$

The parameter c involves a similar sum

$$c = \sum'_{j\Omega} c_{j\Omega} c_{j-(\Omega+1)} (-1)^{j-\frac{1}{2}} [(j-\Omega)(j+\Omega+1)]^{\frac{1}{2}} \quad (11)$$

while

$$\langle K_R^2 \rangle = \sum'_{j\Omega} c_{j\Omega}^2 (K-\Omega)^2 \quad (12)$$

with  $K = \frac{1}{2}$  for  $I = \frac{1}{2}$ . The term  $(A_1 + A_2)d + (A_1 - A_2)e$  has been purposely separated from the main terms in the rotational energy. It has the value

$$\frac{1}{2}(A_1+A_2) \sum'_{j\Omega} c_{j\Omega}^2 \left[ j(j+1) - \Omega^2 + \frac{1}{2} \right] + \frac{1}{2}(A_1-A_2) \sum'_{j\Omega} c_{j\Omega} c_{j(\Omega-2)} \cdot [(j+\Omega)(j-\Omega+1)(j+\Omega-1)(j-\Omega+2)]^{\frac{1}{2}} \quad (13)$$

and is an energy contribution common to all states I. (It arises

from the term  $A_1 j_x^2 + A_2 j_y^2$  in the rotational Hamiltonian, and could in principle be lumped together with the particle energy. In all numerical computations, however, it will be included in the rotational energy.) For  $I > \frac{1}{2}$  matrix elements of the rotational Hamiltonian have been computed between the different possible states  $\Psi_K$  of Eq. (3). They are shown explicitly in Table I for  $I = 3/2$  through  $13/2$  in terms of the rotational constants, the particle parameters  $a$ ,  $b$ , and  $c$ , and the different values of  $\langle K_R^2 \rangle$ . The common term  $(A_1 + A_2)d + (A_1 - A_2)e$  must be added to the rotational energies computed from these matrix elements.

Diagonalization of the  $(I + \frac{1}{2}) \times (I + \frac{1}{2})$  matrices of Table I will yield reliable rotational energies only for particle states which are well separated from other particle excitations since the rotational Hamiltonian, (1), can couple different particle states. In the special case in which two different particle states lie close together the two sets of coupled rotational energies can be obtained from the diagonalization of  $(2I + 1) \times (2I + 1)$  rotational matrices built up from the two coupled  $(I + \frac{1}{2}) \times (I + \frac{1}{2})$  rotational matrices for the different states. Matrix elements diagonal in the particle wave function have the form of Table I, with particle parameters,  $a$ ,  $b$ , etc. defined for each state, and with the two different particle energies added to the diagonal matrix elements. Matrix elements off-diagonal in the particle wave function again have the form of the matrix elements of Table I provided that products of the

TABLE I

Matrix Elements of the Rotational Hamiltonian,  $\langle K' | H_{rot} | K \rangle$

$I = \frac{3}{2}$

	$K = \frac{1}{2}$	$K = -\frac{3}{2}$
$K = \frac{1}{2}$	$(A_1 + A_2)(\frac{3}{2} + a + b) + (A_1 - A_2)c + A_3 \langle K_R^2 \rangle$	$\frac{\sqrt{3}}{2} [(A_1 + A_2)c + (A_1 - A_2)(1 + a + b)]$
$K = -\frac{3}{2}$		$\frac{1}{2}(A_1 + A_2) + A_3 \langle K_R^2 \rangle$

$I = \frac{5}{2}$

	$K = \frac{5}{2}$	$K = \frac{1}{2}$	$K = -\frac{3}{2}$
$K = \frac{5}{2}$	$(A_1 + A_2) + A_3 \langle K_R^2 \rangle$	$\frac{\sqrt{10}}{2} (A_1 - A_2)$	$-\frac{\sqrt{5}}{2} [(A_1 + A_2)(a + b) + (A_1 - A_2)c]$
$K = \frac{1}{2}$		$(A_1 + A_2)[4 - \frac{3}{2}(a + b)] - \frac{3}{2}(A_1 - A_2)c + A_3 \langle K_R^2 \rangle$	$-\sqrt{2}(A_1 + A_2)c + (A_1 - A_2)[\frac{3\sqrt{2}}{2} - \sqrt{2}(a + b)]$
$K = -\frac{3}{2}$			$3(A_1 + A_2) + A_3 \langle K_R^2 \rangle$

$I = \frac{7}{2}$

	$K = \frac{5}{2}$	$K = \frac{1}{2}$	$K = -\frac{3}{2}$	$K = -\frac{7}{2}$
$K = \frac{5}{2}$	$\frac{9}{2}(A_1 + A_2) + A_3 \langle K_R^2 \rangle$	$\frac{3\sqrt{5}}{2} (A_1 - A_2)$	$\sqrt{3}(A_1 + A_2)(a + b) + \sqrt{3}(A_1 - A_2)c$	$\frac{\sqrt{7}}{2} (A_1 - A_2)(a + b) + \frac{\sqrt{7}}{2} (A_1 + A_2)c$
$K = \frac{1}{2}$		$(A_1 + A_2)[\frac{15}{2} + 2(a + b)] + 2(A_1 - A_2)c + A_3 \langle K_R^2 \rangle$	$\frac{\sqrt{15}}{2} (A_1 - A_2)[2 + (a + b)] + \sqrt{15}(A_1 + A_2)c$	0
$K = -\frac{3}{2}$			$\frac{13}{2}(A_1 + A_2) + A_3 \langle K_R^2 \rangle$	$\frac{\sqrt{21}}{2} (A_1 - A_2)$
$K = -\frac{7}{2}$				$\frac{3}{2}(A_1 + A_2) + A_3 \langle K_R^2 \rangle$

Table I (continued)

$$I = \frac{9}{2}$$

	$K = 9/2$	$K = 5/2$	$K = 1/2$	$K = -3/2$	$K = -7/2$
$K = 9/2$	$2(A_1 + A_2) + A_3 \langle K_R^2 \rangle$	$3(A_1 - A_2)$	0	0	$-\frac{3}{2}(A_1 + A_2)(a+b) - \frac{3}{2}(A_1 - A_2)c$
$K = 5/2$		$9(A_1 + A_2) + A_3 \langle K_R^2 \rangle$	$\frac{3\sqrt{7}}{\sqrt{2}}(A_1 - A_2)$	$-\frac{\sqrt{21}}{2}(A_1 + A_2)(a+b) - \frac{\sqrt{21}}{2}(A_1 - A_2)c$	$-2(A_1 - A_2)(a+b) - 2(A_1 + A_2)c$
$K = 1/2$			$(A_1 + A_2)[12 - \frac{5}{2}(a+b)] - \frac{5}{2}(A_1 - A_2)c + A_3 \langle K_R^2 \rangle$	$\sqrt{6}(A_1 - A_2)[\frac{5}{2} - (a+b)] - \sqrt{6}(A_1 + A_2)c$	0
$K = -3/2$				$11(A_1 + A_2) + A_3 \langle K_R^2 \rangle$	$\sqrt{21}(A_1 - A_2)$
$K = -7/2$					$6(A_1 + A_2) + A_3 \langle K_R^2 \rangle$

$$I = \frac{11}{2}$$

	$K = 9/2$	$K = 5/2$	$K = 1/2$	$K = -3/2$	$K = -7/2$	$K = -11/2$
$K = 9/2$	$\frac{15}{2}(A_1 + A_2) + A_3 \langle K_R^2 \rangle$	$\frac{3\sqrt{15}}{2}(A_1 - A_2)$	0	0	$\sqrt{5}(A_1 + A_2)(a+b) + \sqrt{5}(A_1 - A_2)c$	$\frac{\sqrt{11}}{2}(A_1 - A_2)(a+b) + \frac{\sqrt{11}}{2}(A_1 + A_2)c$
$K = 5/2$		$\frac{29}{2}(A_1 + A_2) + A_3 \langle K_R^2 \rangle$	$\sqrt{70}(A_1 - A_2)$	$2\sqrt{2}(A_1 + A_2)(a+b) + 2\sqrt{2}(A_1 - A_2)c$	$\frac{3\sqrt{3}}{2}(A_1 - A_2)(a+b) + \frac{3\sqrt{3}}{2}(A_1 + A_2)c$	0
$K = 1/2$			$(A_1 + A_2)[\frac{35}{2} + 3(a+b)] + 3(A_1 - A_2)c + A_3 \langle K_R^2 \rangle$	$\frac{\sqrt{35}}{2}(A_1 - A_2)[3 + a + b] + \frac{\sqrt{35}}{2}(A_1 + A_2)c$	0	0
$K = -3/2$				$\frac{33}{2}(A_1 + A_2) + A_3 \langle K_R^2 \rangle$	$3\sqrt{6}(A_1 - A_2)$	0
$K = -7/2$					$\frac{23}{2}(A_1 + A_2) + A_3 \langle K_R^2 \rangle$	$\frac{\sqrt{55}}{2}(A_1 - A_2)$
$K = -11/2$						$\frac{5}{2}(A_1 + A_2) + A_3 \langle K_R^2 \rangle$

Table I (continued)

$I = \frac{13}{2}$

	$K = 1\frac{1}{2}$	$K = 9/2$	$K = 5/2$	$K = 1/2$	$K = -3/2$	$K = -7/2$	$K = -11/2$
$K = \frac{13}{2}$	$3(A_1 + A_2) + A_3 \langle K_R^2 \rangle$	$\frac{\sqrt{39}(A_1 - A_2)}{\sqrt{2}}$	$\circ$	$\circ$	$\circ$	$\circ$	$-\frac{\sqrt{13}}{2}(A_1 + A_2)(a+b)$ $-\frac{\sqrt{13}}{2}(A_1 - A_2)c$
$K = \frac{9}{2}$	$14(A_1 + A_2) + A_3 \langle K_R^2 \rangle$	$\frac{\sqrt{165}(A_1 - A_2)}{2}$	$\circ$	$\circ$	$-\frac{\sqrt{33}}{2}(A_1 + A_2)(a+b)$ $-\frac{\sqrt{33}}{2}(A_1 - A_2)c$	$-\frac{\sqrt{6}}{2}(A_1 - A_2)(a+b)$ $-\frac{\sqrt{6}}{2}(A_1 + A_2)c$	
$K = \frac{5}{2}$	$21(A_1 + A_2) + A_3 \langle K_R^2 \rangle$	$3\sqrt{15}(A_1 - A_2)$	$-\frac{3\sqrt{15}}{2}(A_1 + A_2)(a+b)$ $-\frac{3\sqrt{15}}{2}(A_1 - A_2)c$	$-\sqrt{10}(A_1 - A_2)(a+b)$ $-\sqrt{10}(A_1 + A_2)c$	$\circ$		
$K = \frac{1}{2}$		$(A_1 + A_2) \left[ 24 - \frac{7}{2}(a+b) \right]$ $-\frac{7}{2}(A_1 - A_2)c + A_3 \langle K_R^2 \rangle$	$2\sqrt{13}(A_1 - A_2) \left[ \frac{7}{2}(a+b) \right]$ $-2\sqrt{13}(A_1 + A_2)c$	$\circ$	$\circ$		
$K = -\frac{3}{2}$			$23(A_1 + A_2) + A_3 \langle K_R^2 \rangle$	$\frac{15}{\sqrt{2}}(A_1 - A_2)$	$\circ$		
$K = -\frac{7}{2}$				$18(A_1 + A_2) + A_3 \langle K_R^2 \rangle$	$\frac{3\sqrt{11}}{\sqrt{2}}(A_1 - A_2)$		
$K = -\frac{11}{2}$					$9(A_1 + A_2) + A_3 \langle K_R^2 \rangle$		

form  $c_{j\Omega} c_{j\Omega'}$  in the parameters  $a, b, c, d, e$ , and  $\langle K_R^2 \rangle$  are replaced by  $c_{j\Omega}^{(1)} c_{j\Omega'}^{(2)}$  where the superscripts refer to the two different particle states. Terms not proportional to  $a, b$ , etc. must be omitted in matrix elements off-diagonal in the particle states. They are zero through the orthogonality of the different particle wave functions,  $\sum_{j\Omega} c_{j\Omega}^{(1)} c_{j\Omega}^{(2)} = 0$ .

### THE PARTICLE WAVE FUNCTIONS

So far no specific assumptions have been made about the rotational constants, ( $A_k = \hbar^2/2 \mathcal{I}_k$ ), or the particle wave functions describing the odd nucleon. In subsequent calculations the inertial parameters suggested by Bohr's hydrodynamical model<sup>2</sup> will be used

$$\mathcal{I}_k = 4B\beta^2 \sin^2(\gamma - \frac{2\pi}{3}k) \quad (k=1,2,3 = x,y,z) \quad (14)$$

where, however,  $B$  is to be determined empirically. The state of the odd nucleon will be described by wave functions such as those calculated by Newton<sup>5</sup>, that is by the eigenfunctions of a particle in an anisotropic oscillator potential with Nilsson spin-orbit coupling and  $\underline{l}^2$  term. The single particle Hamiltonian is

$$H_{\text{particle}} = -\frac{\hbar^2}{2m} \nabla^2 + \frac{m}{2} (\omega_x X^2 + \omega_y Y^2 + \omega_z Z^2) + C \underline{l} \cdot \underline{s} + D \underline{l}^2 \quad (15)$$

$$\omega_k = \omega_0(\beta, \gamma) \left[ 1 + \sqrt{5/4\pi} \beta \cos(\gamma - \frac{2\pi}{3}k) \right]^{-1} \quad (k=1,2,3 = x,y,z)$$

$$\omega_x \omega_y \omega_z = [\omega_0(\beta = \gamma = 0)]^3 \quad (16)$$



In the notation of Nilsson<sup>6</sup>

$$C = -2 \kappa \hbar \omega_0 \quad D = -\kappa \mu \hbar \omega_0 \quad (17)$$

As pointed out by Nilsson, the eigenfunctions of the Hamiltonian (15) can be treated in two possible ways. The Hamiltonian can be diagonalized by neglecting matrix elements off-diagonal in the principal harmonic oscillator quantum number, N. In this case the particle eigenfunctions are expanded naturally in terms of angular momentum eigenfunctions in real physical space, for example in the  $|N \ell \frac{1}{2} j \Omega\rangle$  representation. Alternately, by introducing the change of variables

$$x = (\hbar/m\omega_x)^{1/2} \xi, \quad y = (\hbar/m\omega_y)^{1/2} \eta, \quad z = (\hbar/m\omega_z)^{1/2} \zeta \quad (18)$$

the single particle Hamiltonian can be made rigorously diagonal in N if the orbital angular momentum operator  $\underline{\ell}$  for the real physical space is replaced by the infinitesimal rotation operator  $\underline{\ell}_{mt}$  in the pseudo-space  $\xi, \eta, \zeta$ , leading to the Hamiltonian

$$H = \frac{\hbar\omega_x}{2} (-\nabla_\xi^2 + \xi^2) + \frac{\hbar\omega_y}{2} (-\nabla_\eta^2 + \eta^2) + \frac{\hbar\omega_z}{2} (-\nabla_\zeta^2 + \zeta^2) + C \underline{\ell}_{mt} \cdot \underline{s} + D \underline{\ell}_{mt}^2 \quad (19)$$

Diagonalization of the Hamiltonian (19) leads to particle eigenfunctions which are expanded in terms of angular momentum eigenfunctions in the pseudo-space  $\xi, \eta, \zeta$ , that is in

an  $|N \ell_t \frac{1}{2} j_t \Omega_t \rangle$  representation. Newton has chosen to diagonalize the Hamiltonian in the form (19). For the present work Newton's calculations have been extended to include the  $N = 5$  and  $6$  harmonic oscillator states and  $N = 4$  states with parameters appropriate for odd- $Z$  nuclei.\* (See Figs. 1 and 2 in this paper and Mottelson and Nilsson, reference 9.) The particle wave functions are therefore known in the form of Eq. (2), but as linear combinations of angular momentum eigenfunctions in the pseudo-space  $\xi, \eta, \zeta$ . The formulae for the rotational energies, on the other hand, as well as all subsequent formulae for electromagnetic moments and transition probabilities, particle widths, etc. are given in terms of expansion coefficients involving the angular momentum eigenfunctions in real physical space. To first order in  $\sqrt{5/4\pi} \beta$ , however, the two types of functions are identical. Since the model can be expected to have approximate validity, at best, no

\*The diagonalization of the Hamiltonian (19) was carried out on the IBM 704 digital computer of The University of Michigan Computing Center. The problem has been programmed for arbitrary values of  $C, D, \beta$ , and  $\uparrow$  and computes the eigenvalues and eigenvectors as well as parameters such as  $a, b$ , etc. and some additional quantities which are useful in the computation of electromagnetic moments and transition probabilities. The diagonalization of the  $(I + \frac{1}{2}) \times (I + \frac{1}{2})$  rotational matrices (with  $I \leq 13/2$ ) was also carried out on the IBM 704 computer.

distinction will be made between the two types of eigenfunctions.

If the distinction were to be taken literally, the operator  $j_x$  in the rotational Hamiltonian, for example, could be written

$$j_x = s_x + l_x = s_x + \frac{1}{2} \left( \sqrt{\frac{\omega_z}{\omega_y}} - \sqrt{\frac{\omega_y}{\omega_z}} \right) (\eta p_\xi + \zeta p_\eta) + \frac{1}{2} \left( \sqrt{\frac{\omega_z}{\omega_y}} + \sqrt{\frac{\omega_y}{\omega_z}} \right) (\eta p_\xi - \zeta p_\eta)$$

The second term can be ignored since it has no matrix elements diagonal in  $N$  while the eigenfunctions of the Hamiltonian (19) are rigorously diagonal in  $N$ . Therefore  $j_x$  could be replaced by

$$j_x = s_x + (1+h) l_{tx} = j_{tx} + h l_{tx}$$

where 
$$h = \frac{1}{2} \left( \sqrt{\frac{\omega_z}{\omega_y}} + \sqrt{\frac{\omega_y}{\omega_z}} \right) - 1$$

In the most unfavorable case, ( $\theta = 30^\circ$ ),  $h$  would have the value

$$h = (15/8\pi) \beta^2 + \text{order}(\beta^4)$$

Insofar as  $h$  can be neglected the matrix elements of  $j_x$  are independent of the choice of eigenfunctions, and no distinction need be made between the  $|N l \frac{1}{2} j \Omega\rangle$  and the  $|N l_{t \frac{1}{2}} j_t \Omega_t\rangle$  representations.

#### ELECTROMAGNETIC MOMENTS. TRANSITION PROBABILITIES

Expressions for the electromagnetic moments and transition probabilities are straightforward generalizations of the expressions developed for axially symmetric nuclei.<sup>2,6,10,11</sup> They involve matrix elements of the multipole operators,  $\mathcal{M}(L, \mu)$ ,

between the possible states  $\psi_K$  of Eq. (3) and summations over the coefficients  $C_K$ . The reduced transition probability between states  $I_i$  and  $I_f$ , governed by an arbitrary tensor operator of rank  $L$ , is defined as usual by

$$B(L, I_i \rightarrow I_f) = \sum_{\mu, M_f} |\langle \alpha_f I_f M_f | \mathcal{M}(L, \mu) | \alpha_i I_i M_i \rangle|^2 \quad (20)$$

The  $\mu^{\text{th}}$  space-fixed spherical component of the tensor operator is given in terms of the body-fixed components  $\mathcal{M}'(L, \nu)$  by  $\mathcal{M}(L, \mu) = \sum_{\nu} D_{\mu\nu}^L \mathcal{M}'(L, \nu)$ . If the tensor operator is a function of the odd nucleon's intrinsic coordinates the reduced transition probability can be written

$$B(L, I_i \rightarrow I_f) = \left[ \sum_{j_i, j_f} \sum'_K \sum'_\Omega \langle j_f || \mathcal{M}'(L) || j_i \rangle (2j_f + 1)^{-1/2} \cdot \left\{ \sum_{\text{even } \nu} C_K^{(i)} C_{(K+\nu)}^{(f)} C_{j_i \Omega}^{(i)} C_{j_f(\Omega+\nu)}^{(f)} \langle I_i L K \nu | I_i L I_f(K+\nu) \rangle \langle j_i L \Omega \nu | j_i L j_f(\Omega+\nu) \rangle + \sum_{\text{odd } \nu} C_K^{(i)} C_{-(K+\nu)}^{(f)} C_{j_i \Omega}^{(i)} C_{j_f(-\Omega+\nu)}^{(f)} (-1)^{I_f - j_f} \langle I_i L K \nu | I_i L I_f(K+\nu) \rangle \langle j_i L \Omega \nu | j_i L j_f(\Omega+\nu) \rangle \right\} \right]^2 \quad (21)$$

As previously, the prime on the summation symbols indicates that the sums over  $K$  and  $\Omega$  are restricted to the set of values  $\dots -\frac{7}{2}, -\frac{3}{2}, \frac{1}{2}, \frac{5}{2}, \frac{9}{2}, \dots$ . Only the value of the reduced matrix element of the particle operator of rank  $L$  remains to be calculated. The above formula can be applied specifically if the particle wave functions are expanded in the form of Eq. (2), that is in the  $|N e \frac{1}{2} j \Omega \rangle$  representation. For some types of operators the  $|N e \Lambda \frac{1}{2} \Sigma \rangle$  representation used by Nilsson may

lead to simpler expressions for the reduced transition probabilities. The quantum numbers  $\Lambda$  and  $\Sigma$  give the eigenvalues of  $l_z$  and  $s_z$ , the body-fixed z components of the orbital and spin angular momentum of the odd nucleon, in units of  $\hbar$ . The Nilsson expansion coefficients  $a_{\ell\Lambda\Sigma}$  are given in terms of the  $c_{j\Omega}$  through\*

$$a_{\ell\Lambda\Sigma} = \sum_j \langle \ell \frac{1}{2} \Lambda \Sigma | \ell \frac{1}{2} j \Omega \rangle c_{j\Omega}$$

In terms of such coefficients an alternate expression for the reduced transition probability may be useful

$$\begin{aligned} B(L, I_i \rightarrow I_f) = & \left[ \sum_{\alpha_i \alpha_f} \sum_K \sum_{\Omega} \left\{ \sum_{\text{even } \nu} C_K^{(i)} C_{(K+\nu)}^{(f)} a_{\alpha_i \Omega}^{(i)} a_{\alpha_f (\Omega+\nu)}^{(f)} \langle I_i L K \nu | I_i L I_f (K+\nu) \rangle \langle \alpha_f (\Omega+\nu) | m'(L, \nu) | \alpha_i \Omega \rangle \right. \right. \\ & \left. \left. + \sum_{\text{odd } \nu} C_K^{(i)} C_{-(K+\nu)}^{(f)} a_{\alpha_i \Omega}^{(i)} a_{\alpha_f -(\Omega+\nu)}^{(f)} (-1)^{I_f - \frac{1}{2}} \langle I_i L K \nu | I_i L I_f (K+\nu) \rangle \langle \alpha_f (\Omega+\nu) | m'(L, \nu) | \alpha_i \Omega \rangle \right\} \right]^2 \end{aligned} \quad (22)$$

where the labels  $\alpha$  stand collectively for quantum numbers such as  $N, \ell, \Lambda$ , and  $\Sigma$ .

\*In order to define the phases of the coefficients it is important to note that the  $c_{j\Omega}$  are defined in the  $|N \ell \frac{1}{2} j \Omega \rangle$  rather than in the  $|N \frac{1}{2} \ell j \Omega \rangle$  representation. The quantum numbers  $N, \ell$ , and  $s = \frac{1}{2}$  are never indicated in  $c_{j\Omega}$  but are to be implicitly understood.

The expression for the magnetic moment takes the specific form

$$\begin{aligned} \mu = & g_R I + \frac{1}{(I+1)} \sum'_K C_K^2 K \left[ (g_s - g_e) \langle s_0 \rangle + (g_e - g_e) \langle \Omega \rangle \right] \\ & + \sum'_K C_K C_{-(K-1)} (-1)^{I-1/2} \frac{[(I+K)(I-K+1)]^{1/2}}{2(I+1)} \left[ (g_s - g_e) \langle s_- \rangle + (g_e - g_e) (a+b) \right] \\ & + \sum'_K C_K C_{-(K+1)} (-1)^{I-1/2} \frac{[(I-K)(I+K+1)]^{1/2}}{2(I+1)} \left[ (g_s - g_e) \langle s_+ \rangle + (g_e - g_e) c \right] \end{aligned} \quad (23)$$

where (a + b) and c are written out explicitly in Eqs. (10) and (11), while  $\langle \Omega \rangle = \sum'_{j\Omega} c_{j\Omega}^2 \Omega$ . Expectation values such as  $\langle s_0 \rangle$  have their simplest form in terms of the expansion coefficients  $a_{\ell\Lambda\Sigma}$

$$\begin{aligned} \langle s_0 \rangle &= \frac{1}{2} \sum_{\ell} \sum'_{\Omega} \left( a_{\ell(\Omega-1/2)1/2}^2 - a_{\ell(\Omega+1/2)-1/2}^2 \right) \\ \langle s_- \rangle &= \sum_{\ell} \sum'_{\Omega} (-1)^{\ell} a_{\ell(\Omega-1/2)1/2} a_{\ell-(\Omega-1/2)1/2} \\ \langle s_+ \rangle &= \sum_{\ell} \sum'_{\Omega} (-1)^{\ell} a_{\ell(\Omega+1/2)-1/2} a_{\ell-(\Omega+1/2)-1/2} \end{aligned} \quad (24)$$

The electric quadrupole moment is given by

$$\begin{aligned} Q_s = & (Q_0 \cos \gamma + q_0) \sum'_K C_K^2 \frac{[3K^2 - I(I+1)]}{(I+1)(2I+3)} \\ & + (Q_0 \sin \gamma + q_2) \sum'_K C_K C_{(K-2)} \frac{[3(I+K)(I+K-1)(I-K+1)(I-K+2)]^{1/2}}{(I+1)(2I+3)} \end{aligned} \quad (25)$$

where  $Q_0$  gives the contribution of the deformed core

$$Q_0 = 3Z e R_0^2 \beta / \sqrt{5\pi} \quad (26)$$

while  $q_0$  and  $q_2$  give the contribution of the odd nucleon. The matrix elements of  $e_p r_p^2 Y_{2\mu}(\theta_p)$  for the odd particle are again evaluated most easily in terms of the expansion coefficients  $a_{\ell\Lambda\Sigma}$  and lead to

$$q_0 = \frac{2e_p \hbar}{m\omega_0} \sum_{\ell\Lambda} \left[ -a_{\ell\Lambda}^2 \left(N + \frac{3}{2}\right) \left[ \frac{\ell(\ell+1)}{(2\ell-1)(2\ell+3)} \right]^{\frac{1}{2}} \langle \ell 2 \Lambda 0 | \ell 2 \ell \Lambda \rangle \right. \\ \left. + 2a_{\ell\Lambda} a_{(\ell-2)\Lambda} \left[ \frac{(N+\ell+1)(N-\ell+2)3\ell(\ell-1)}{2(2\ell-1)(2\ell-3)} \right]^{\frac{1}{2}} \langle \ell 2 \Lambda 0 | \ell 2 (\ell-2) \Lambda \rangle \right]$$

$$q_2 = \frac{2e_p \hbar}{m\omega_0} \sum_{\ell\Lambda} \left[ -a_{\ell\Lambda} a_{\ell(\Lambda+2)} \left(N + \frac{3}{2}\right) \left[ \frac{\ell(\ell+1)}{(2\ell-1)(2\ell+3)} \right]^{\frac{1}{2}} \langle \ell 2 \Lambda 2 | \ell 2 \ell (\Lambda+2) \rangle \right. \\ \left. + a_{\ell\Lambda} a_{(\ell-2)(\Lambda+2)} \left[ \frac{(N+\ell+1)(N-\ell+2)3\ell(\ell-1)}{(2\ell-1)(2\ell-3)} \right]^{\frac{1}{2}} \langle \ell 2 \Lambda 2 | \ell 2 (\ell-2) (\Lambda+2) \rangle \right]^{(27)} \\ \left. + a_{\ell\Lambda} a_{(\ell+2)(\Lambda+2)} \left[ \frac{(N+\ell+3)(N-\ell)3(\ell+2)(\ell+1)}{(2\ell+3)(2\ell+5)} \right]^{\frac{1}{2}} \langle \ell 2 \Lambda 2 | \ell 2 (\ell+2) (\Lambda+2) \rangle \right]$$

The quantum number  $\Sigma$ , (as well as the harmonic oscillator quantum number,  $N$ ), is not indicated explicitly in the coefficients  $a_{\ell\Lambda}$  since all the matrix elements are diagonal in  $\Sigma$ . ( $e_p$  is the charge of the odd nucleon. An effective charge might be used if vibrational interactions with the core are taken into account.) It should be noted that  $Q_s$  can be negative even if

the nucleus has a large positive intrinsic deformation, ( $\beta > 0$ ,  $\gamma \leq 30^\circ$ ).

Since explicit expressions for M1 and E2 reduced transition probabilities may be useful, they are tabulated below for transitions  $I_i \rightarrow I_f$  between different rotational states based on the same particle excitation

$$\begin{aligned}
 B(M1, I_i \rightarrow I_f) = & \frac{3}{4\pi} \left[ g_R [I_i(I_i+1)]^{\frac{1}{2}} \delta_{I_i I_f} \sum_K C_K^{(i)} C_K^{(f)} \right. \\
 & + \sum_K C_K^{(i)} C_K^{(f)} \langle I_i | K0 | I_i | I_f K \rangle \left\{ (g_s - g_e) \langle s_0 \rangle + (g_e - g_R) \langle \Omega \rangle \right\} \\
 & + \sum_K C_K^{(i)} C_{-(K-1)}^{(f)} \langle I_i | K-1 | I_i | I_f (K-1) \rangle \frac{(-1)^{I_f - \frac{1}{2}}}{\sqrt{2}} \left\{ (g_s - g_e) \langle s_- \rangle + (g_e - g_R) (a+b) \right\} \\
 & + \sum_K C_K^{(i)} C_{-(K+1)}^{(f)} \langle I_i | K1 | I_i | I_f (K+1) \rangle \frac{(-1)^{I_f + \frac{1}{2}}}{\sqrt{2}} \left\{ (g_s - g_e) \langle s_+ \rangle + (g_e - g_R) c \right\} \left. \right]^2
 \end{aligned} \tag{28}$$

(If there is a change in the particle excitation of the odd nucleon in the transition, the expressions for the M1 transition probabilities are merely slight generalizations of the above formula which are obtained if products of the form  $c_{j\Omega} c_{j-(\Omega-1)}$  and  $a_{e(\Omega-\frac{1}{2})\frac{1}{2}} a_{e-(\Omega-\frac{1}{2})\frac{1}{2}}$  in the expectation values are replaced by  $c_{j\Omega}^{(i)} c_{j-(\Omega-1)}^{(f)}$  and  $a_{e(\Omega-\frac{1}{2})\frac{1}{2}}^{(i)} a_{e-(\Omega-\frac{1}{2})\frac{1}{2}}^{(f)}$ , respectively.)

The E2 rates, again for transitions between different rotational states based on the same particle excitation, are given by



$$B(E2, I_i \rightarrow I_f) = \frac{5}{16\pi} \left[ (Q_0 \cos \theta + q_0) \sum_K C_K^{(i)} C_K^{(f)} \langle I_i 2K0 | I_f 2I_f K \rangle \right. \\ \left. + \frac{(Q_0 \sin \theta + q_2)}{\sqrt{2}} \sum_K \left( C_K^{(i)} C_{(K-2)}^{(f)} \langle I_i 2K-2 | I_f 2I_f(K-2) \rangle + C_K^{(i)} C_{(K+2)}^{(f)} \langle I_i 2K2 | I_f 2I_f(K+2) \rangle \right) \right]^2 \quad (29)$$

(If the transition involves a change in the particle excitation, the core can give no contribution. The contributions of the odd nucleon will have a more complicated form and will involve five different terms of the form  $q_2, q_{-2}, q_1, q_{-1},$  and  $q_0$ .)

#### SPECTROSCOPIC FACTORS FOR NUCLEON EMISSION OR CAPTURE

In this section we consider the relative amplitudes for nucleon capture into, or removal from, bound states of asymmetric nuclei. Such amplitudes are measured by stripping and pick-up reactions, respectively<sup>12</sup>. The amplitude for stripping or pick-up contains an overlap integral over target and residual nucleus wave functions, which may be expanded in the form

$$\int \psi_{A+1}^*(\xi, \underline{x}) \psi_A(\xi) d\xi = \sum_j \beta_j \langle I_{Aj} M_A m | I_{Aj} I_{A+1} M_{A+1} \rangle \chi_m^j(\underline{x}) \quad (30)$$

$\underline{x}$  denotes the coordinates of the  $(A + 1)$ th nucleon, while the  $z$ -component  $m$  refers to a space-fixed coordinate system.

Quantum numbers such as  $N$  and  $\ell$  are not explicitly indicated

in (30) for simplicity. The parentage coefficient  $\beta_j$ , in expansion (30) is then the amplitude for finding the  $(A + 1)$ th. nucleon with angular momentum  $j$  within the nucleus of mass  $A + 1$  when in a state  $\tilde{\psi}_{A+1}$ , with the remaining nucleus of mass  $A$  in state  $\psi_A$ . If there are  $n$  nucleons of this type in nucleus  $(A + 1)$ , the capture or emission probability is proportional to the spectroscopic factor<sup>12</sup>,

$$S(j) = n |\beta_j|^2 \quad (31)$$

The two cases we shall consider are the removal of a nucleon from (i) an odd- $A$  nucleus to leave an even nucleus, and (ii) an even nucleus to leave an odd- $A$  nucleus. (The stripping processes are simply the inverses.) In previous sections we have only considered the states of a nucleus with a single nucleon coupled to a structureless asymmetric core. This is adequate for the description of the removal of the nucleon if the core is identified with the resulting even nucleus. However, the removal of a nucleon from an even nucleus requires a more detailed description. One simple generalization is to consider the nucleons to fill (consistently with the Pauli Principle) the lowest levels in the ellipsoidal single-particle potential well. If we restrict ourselves to configurations in which even numbers of nucleons are paired off in the lowest (doubly degenerate) single-particle levels while only the last odd particle is allowed

to change its state, it is straightforward to show that the resulting energy levels and wave functions are the same as for the single-particle model of the preceding sections. (This simple equivalence does not hold for more complicated configurations.) The other nucleons merely form an inert core which we assume to be the same as the corresponding even nucleus. However, we now have a consistent mechanism for removal of a nucleon from an even nucleus, or inversely its addition to an odd-A nucleus.

With this assumption, the wave-function of the even nucleus now has the form

$$\Psi_e = \sqrt{\frac{2I_e+1}{16\pi^2}} \sum_{K_e} C_{K_e} \left[ D_{M_{K_e}}^{I_e} + (-1)^{I_e} D_{M_{-K_e}}^{I_e} \right] \mathbf{X} \quad (32)$$

The summation is over positive, even values of  $K_e$  only, including zero, and  $C_0$  is chosen to absorb a factor of  $\sqrt{2}$  which arises because the normalization of the function in brackets is different for the special case  $K_e = 0$ . The  $\mathbf{X}$  is a normalized determinant of the wave functions (2) for the occupied single-particle states\*. The odd-A nucleus has a wave function which

\* If neutrons and protons are treated as distinguishable,  $\mathbf{X}$  is a product of determinants, of order  $N$  for the neutrons and of order  $Z$  for the protons.

is a generalization of (3),

$$\Psi_0 = \sqrt{\frac{2I_0+1}{16\pi^2}} \sum_{K_0}' C_{K_0} \left[ D_{M_0 K_0}^{I_0} \underline{X}_{\nu} + (-1)^{I_0-1/2} D_{M_0-K_0}^{I_0} \underline{X}_{-\nu} \right] \quad (33)$$

The  $\underline{X}_{\nu}$  is again a determinant of single-particle states. For the configurations which we are considering, all but one of the nucleons are paired off, while the odd one occupies the state  $\mathcal{X}_{\nu}$ . The  $\underline{X}_{-\nu}$  is similar but with the odd nucleon in the state  $\mathcal{X}_{-\nu}$ .

With these wave-functions the amplitudes  $\beta$  from the overlap (30) are given by

Case 1: A = even nucleus (e); (A + 1) = odd nucleus (o)

$$\sqrt{n} \beta_j = \sqrt{\frac{2I_e+1}{2I_0+1}} \sum_{K_e}' \sum_{K_0}' C_{K_e}^{(A)} C_{K_0}^{(A+1)} \left[ c_{j(K_0-K_e)} \langle I_e j K_e (K_0-K_e) | I_e j I_0 K_0 \rangle \right. \\ \left. + (-1)^{I_e} c_{j(K_0+K_e)} \langle I_e j -K_e (K_0+K_e) | I_e j I_0 K_0 \rangle \right] \quad (34)$$

Case 2: A = odd nucleus (o); (A + 1) = even nucleus (e)

$$\sqrt{n} \beta_j = \sqrt{\frac{2I_0+1}{2I_e+1}} \sum_{K_0}' \sum_{K_e}' C_{K_0}^{(A)} C_{K_e}^{(A+1)} (-1)^{j-1/2} \left[ c_{j(K_0-K_e)} \langle I_0 j K_0 (K_e-K_0) | I_0 j I_e K_e \rangle \right. \\ \left. + (-1)^{I_e} c_{j(K_0+K_e)} \langle I_0 j K_0 -(K_e+K_0) | I_0 j I_e -K_e \rangle \right] \quad (35)$$

where n in (34) or (35) is the number of nucleons in (A + 1) of the same type as the one removed.

The spectroscopic factor is then  $S(j) = |\sqrt{n} \beta_j|^2$ .

## NUMERICAL RESULTS. POSSIBLE APPLICATIONS

According to our model the odd-A nucleus is assumed to have a well defined asymmetric equilibrium shape. In looking for possible examples for such a model the neighboring even-even nuclei might be used as a guide. Preferably these should have large asymmetry and show relatively little vibration-rotation interaction. There is some indication that nuclei around  $A \approx 190$  may satisfy both requirements. Asymmetries of  $16.5^\circ$ ,  $19^\circ$ ,  $22^\circ$ , and  $25^\circ$  have been reported<sup>3</sup> for the sequence  $Os^{186}$ ,  $Os^{188}$ ,  $Os^{190}$ , and  $Os^{192}$ , for example; and the indications are that asymmetric rotator theory is satisfactory, particularly for the isotopes  $Os^{190}$  and  $Os^{192}$ . For this reason it was decided to make a preliminary survey of the odd-A nuclei around  $A \approx 190$ . Unfortunately very little is known about the excited states of the odd-A isotopes of osmium, although it might be noted that the experimentally observed magnetic moment of  $Os^{187}$  ( $\mu = .12$ ) is considerably smaller than the value predicted on the basis of an axially symmetric rotator model ( $\mu = .8$ , Table VII, Mottelson and Nilsson, reference 9). Although insufficient experimental information is available for a test of asymmetric rotator theory in the case of  $Os^{187}$  and  $Os^{189}$ , the experimental situation is somewhat more favorable in the case of some of the isotopes of Re, Ir, Au, Pt, and perhaps W.

## ODD Z NUCLEI

The low-lying levels of the isotopes of Re seem to form

a  $5/2+$ ,  $7/2+$ ,  $9/2+$  rotational sequence. The various isotopes of Ir and Au all have  $3/2+$  ground states with magnetic moments between .1 and .2 nuclear magnetons. On the basis of an axially symmetric model rotational bands based on  $\Omega = \frac{5}{2}+$  and  $\frac{3}{2}+$  states should be expected in these two cases. The most likely particle states are the  $[402] \Omega = \frac{5}{2}+$  Nilsson level for the 75<sup>th</sup> proton in Re and the  $[402] \Omega = \frac{3}{2}+$  Nilsson level for the 77<sup>th</sup> and 79<sup>th</sup> protons in Ir and Au. (See Fig. 3, Mottelson and Nilsson, reference 9. The levels are labeled by the asymptotic quantum numbers  $[N n_z \Lambda]$  .) In an asymmetric nucleus  $\Omega$  is no longer a good quantum number. With the introduction of a small asymmetry Nilsson levels with different  $\Omega$  interact with each other. As a result the single particle levels of an asymmetric nucleus cannot cross each other when plotted as a function of the deformation parameter  $\beta$ , except for states of opposite parity. For small values of the asymmetry parameter,  $\gamma$ , the single particle energies differ little from the Nilsson values, except in regions where Nilsson levels with different  $\Omega$  cross each other or lie close together over large ranges of  $\beta$ . The single particle levels for asymmetric odd Z nuclei in the region  $50 < Z < 82$  are shown in Figure 1. for an intermediate value of the asymmetry parameter,  $\gamma = 15^\circ$  and in Figure 2. for the largest possible asymmetry,  $\gamma = 30^\circ$ . In order to give some idea of the possible rotational bands which can be built on these particle states, the levels have been labeled with the spin of the ground state, (lowest rotational level), for  $\beta$  values of

-.2, and .3. For these specific values of  $\beta$  and  $\gamma$  the spin values of the lowest rotational levels based on each particle state are also listed in Table II starting with the ground state at the left. Since the rotational spin sequences may be very sensitive functions of both  $\beta$  and  $\gamma$ , the spin values listed in Table II can only serve as an indication of the types of rotational sequences to be expected. The investigation of any specific example must be based on a plot of the rotational energies as a function of  $\gamma$  for appropriate values of  $\beta$ .

To get some understanding of the behavior of the rotational levels, however, consider particle state 65, the lowest negative parity single-particle state which grows out of the  $h_{11/2}$  shell model level, as an example. In the prolate symmetric rotator limit,  $\beta > 0$ ,  $\gamma = 0^\circ$ , this is a pure  $\Omega = \frac{1}{2}$  state with an  $I = 3/2$  rotational ground state. In the oblate symmetric rotator limit,  $\beta < 0$ ,  $\gamma = 0^\circ$ , or what is equivalent,  $\beta > 0$ ,  $\gamma = 60^\circ$ , this is a pure  $\Omega = 11/2$  state with an  $I = 11/2$  rotational ground state. Between  $\gamma$  of  $0^\circ$  and  $60^\circ$  ( $\beta > 0$ ) the ground state therefore changes from an  $I = 3/2$  to an  $I = 11/2$  state. Note, however, that for  $\gamma = 30^\circ$  an  $I = 11/2$  value has already been reached, whereas for  $\gamma = 15^\circ$  the ground state  $I$  value is  $7/2$ . Note also from Figure 2 that  $I = \frac{1}{2}$  ground states are very common in the case of large asymmetry. Although the single particle levels could be labeled with the asymptotic quantum numbers  $[n_x n_y n_z]$  this does not seem to be a useful label since the order of the single particle levels  $[n_x n_y n_z]$  would be a function of  $\gamma$ .

TABLE II

Order of Low-Lying Rotational Levels for Odd-Z Nuclei

$\beta = .3 \quad \gamma = 15^\circ$

Particle State	Pa- rity	Spins of Lowest Rotational States						Particle State	Pa- rity	Spins of Lowest Rotational States					
		↓ Ground State								↓ Ground State					
93	-	$\frac{1}{2}$	$\frac{3}{2}$	$\frac{5}{2}$	$\frac{7}{2}$	$\frac{9}{2}$	$\frac{11}{2}$ ...	61	+	$\frac{1}{2}$	$\frac{3}{2}$	$\frac{5}{2}$	$\frac{7}{2}$	$\frac{9}{2}$	$\frac{3}{2}$ ...
81	+	$\frac{1}{2}$	$\frac{3}{2}$	$\frac{5}{2}$	$\frac{3}{2}$	$\frac{7}{2}$	$\frac{5}{2}$ ...	73	-	$\frac{1}{2}$	$\frac{5}{2}$	$\frac{3}{2}$	$\frac{9}{2}$	$\frac{7}{2}$	$\frac{11}{2}$ ...
91	-	$\frac{1}{2}$	$\frac{3}{2}$	$\frac{5}{2}$	$\frac{7}{2}$	$\frac{9}{2}$	$\frac{5}{2}$ ...	71	-	$\frac{7}{2}$	$\frac{9}{2}$	$\frac{11}{2}$	$\frac{3}{2}$	$\frac{5}{2}$	$\frac{7}{2}$ ...
89	-	$\frac{11}{2}$	$\frac{7}{2}$	$\frac{9}{2}$	$\frac{11}{2}$	...		59	+	$\frac{1}{2}$	$\frac{3}{2}$	$\frac{5}{2}$	$\frac{7}{2}$	$\frac{9}{2}$	$\frac{3}{2}$ ...
87	-	$\frac{1}{2}$	$\frac{3}{2}$	$\frac{5}{2}$	$\frac{7}{2}$	$\frac{9}{2}$	$\frac{3}{2}$ ...	57	+	$\frac{1}{2}$	$\frac{3}{2}$	$\frac{5}{2}$	$\frac{7}{2}$	$\frac{9}{2}$	$\frac{5}{2}$ ...
79	+	$\frac{1}{2}$	$\frac{3}{2}$	$\frac{3}{2}$	$\frac{5}{2}$	$\frac{5}{2}$	$\frac{7}{2}$ ...	69	-	$\frac{5}{2}$	$\frac{7}{2}$	$\frac{9}{2}$	$\frac{11}{2}$	$\frac{1}{2}$	$\frac{3}{2}$ ...
85	-	$\frac{3}{2}$	$\frac{5}{2}$	$\frac{1}{2}$	$\frac{3}{2}$	$\frac{7}{2}$	$\frac{9}{2}$ ...	55	+	$\frac{9}{2}$	$\frac{5}{2}$	$\frac{7}{2}$	$\frac{9}{2}$	...	
83	-	$\frac{9}{2}$	$\frac{11}{2}$	$\frac{5}{2}$	$\frac{7}{2}$	$\frac{9}{2}$	$\frac{11}{2}$ ...	53	+	$\frac{1}{2}$	$\frac{3}{2}$	$\frac{5}{2}$	$\frac{7}{2}$	$\frac{3}{2}$	$\frac{5}{2}$ ...
77	+	$\frac{1}{2}$	$\frac{3}{2}$	$\frac{5}{2}$	$\frac{7}{2}$	$\frac{9}{2}$	$\frac{5}{2}$ ...	67	-	$\frac{3}{2}$	$\frac{5}{2}$	$\frac{7}{2}$	$\frac{9}{2}$	$\frac{11}{2}$	$\frac{1}{2}$ ...
75	-	$\frac{1}{2}$	$\frac{3}{2}$	$\frac{3}{2}$	$\frac{5}{2}$	$\frac{5}{2}$	$\frac{7}{2}$ ...	51	+	$\frac{3}{2}$	$\frac{1}{2}$	$\frac{5}{2}$	$\frac{3}{2}$	$\frac{5}{2}$	$\frac{7}{2}$ ...
63	+	$\frac{3}{2}$	$\frac{5}{2}$	$\frac{7}{2}$	$\frac{9}{2}$	$\frac{7}{2}$	$\frac{9}{2}$ ...	65	-	$\frac{7}{2}$	$\frac{11}{2}$	$\frac{3}{2}$	$\frac{1}{2}$	$\frac{5}{2}$	$\frac{9}{2}$ ...



Table II (continued)

Order of Low-Lying Rotational Levels for Odd-Z Nuclei

$\beta = -.2 \quad \gamma = 15^\circ$

Particle State	Pa- rity	Spins of Lowest Rotational States						Particle State	Pa- rity	Spins of Lowest Rotational States					
		Ground State								Ground State					
81	+	$\frac{1}{2}$	$\frac{3}{2}$	$\frac{5}{2}$	$\frac{7}{2}$	$\frac{9}{2}$	$\frac{3}{2}$ ...	71	-	$\frac{3}{2}$	$\frac{5}{2}$	$\frac{7}{2}$	$\frac{1}{2}$	$\frac{7}{2}$	$\frac{11}{2}$ ...
93	-	$\frac{1}{2}$	$\frac{3}{2}$	$\frac{5}{2}$	$\frac{7}{2}$	$\frac{9}{2}$	$\frac{3}{2}$ ...	63	+	$\frac{1}{2}$	$\frac{3}{2}$	$\frac{5}{2}$	$\frac{7}{2}$	$\frac{9}{2}$	$\frac{3}{2}$ ...
91	-	$\frac{5}{2}$	$\frac{7}{2}$	$\frac{9}{2}$	$\frac{1}{2}$	$\frac{3}{2}$	$\frac{11}{2}$ ...	69	-	$\frac{7}{2}$	$\frac{9}{2}$	$\frac{11}{2}$	$\frac{3}{2}$	$\frac{5}{2}$	$\frac{7}{2}$ ...
89	-	$\frac{7}{2}$	$\frac{9}{2}$	$\frac{3}{2}$	$\frac{11}{2}$	$\frac{5}{2}$	$\frac{7}{2}$ ...	61	+	$\frac{3}{2}$	$\frac{5}{2}$	$\frac{1}{2}$	$\frac{3}{2}$	$\frac{7}{2}$	$\frac{5}{2}$ ...
87	-	$\frac{1}{2}$	$\frac{3}{2}$	$\frac{5}{2}$	$\frac{9}{2}$	$\frac{7}{2}$	$\frac{5}{2}$ ...	59	+	$\frac{3}{2}$	$\frac{1}{2}$	$\frac{5}{2}$	$\frac{3}{2}$	$\frac{7}{2}$	$\frac{9}{2}$ ...
85	-	$\frac{7}{2}$	$\frac{9}{2}$	$\frac{11}{2}$	$\frac{3}{2}$	$\frac{5}{2}$	$\frac{7}{2}$ ...	57	+	$\frac{5}{2}$	$\frac{7}{2}$	$\frac{9}{2}$	$\frac{1}{2}$	$\frac{3}{2}$	$\frac{5}{2}$ ...
83	-	$\frac{9}{2}$	$\frac{11}{2}$	$\frac{5}{2}$	$\frac{7}{2}$	$\frac{9}{2}$	$\frac{11}{2}$ ...	67	-	$\frac{9}{2}$	$\frac{11}{2}$	$\frac{5}{2}$	$\frac{7}{2}$	$\frac{9}{2}$	$\frac{11}{2}$ ...
79	+	$\frac{1}{2}$	$\frac{3}{2}$	$\frac{5}{2}$	$\frac{7}{2}$	$\frac{3}{2}$	$\frac{9}{2}$ ...	55	+	$\frac{3}{2}$	$\frac{5}{2}$	$\frac{1}{2}$	$\frac{7}{2}$	$\frac{3}{2}$	$\frac{5}{2}$ ...
75	-	$\frac{7}{2}$	$\frac{11}{2}$	$\frac{3}{2}$	$\frac{9}{2}$	$\frac{5}{2}$	$\frac{1}{2}$ ...	53	+	$\frac{5}{2}$	$\frac{7}{2}$	$\frac{9}{2}$	$\frac{1}{2}$	$\frac{3}{2}$	$\frac{5}{2}$ ...
77	+	$\frac{3}{2}$	$\frac{5}{2}$	$\frac{7}{2}$	$\frac{1}{2}$	$\frac{3}{2}$	$\frac{9}{2}$ ...	65	-	$\frac{11}{2}$	$\frac{7}{2}$	$\frac{9}{2}$	$\frac{11}{2}$	...	
73	-	$\frac{5}{2}$	$\frac{9}{2}$	$\frac{1}{2}$	$\frac{3}{2}$	$\frac{7}{2}$	$\frac{11}{2}$ ...	51	+	$\frac{7}{2}$	$\frac{9}{2}$	$\frac{3}{2}$	$\frac{5}{2}$	$\frac{7}{2}$	$\frac{9}{2}$ ...

Table II (continued)

Order of Low-Lying Rotational Levels for Odd-Z Nuclei

$\beta = .3$								$\gamma = 30^\circ$									
Particle State	Pa- rity	Spins of Lowest Rotational States						...	Particle State	Pa- rity	Spins of Lowest Rotational States						...
		Ground State									Ground State						
81	+	$\frac{1}{2}$	$\frac{3}{2}$	$\frac{5}{2}$	$\frac{3}{2}$	$\frac{5}{2}$	$\frac{7}{2}$	...	73	-	$\frac{5}{2}$	$\frac{9}{2}$	$\frac{7}{2}$	$\frac{1}{2}$	$\frac{11}{2}$	$\frac{3}{2}$	...
95	-	$\frac{1}{2}$	$\frac{3}{2}$	$\frac{3}{2}$	$\frac{5}{2}$	$\frac{7}{2}$	$\frac{9}{2}$	...	61	+	$\frac{3}{2}$	$\frac{1}{2}$	$\frac{5}{2}$	$\frac{3}{2}$	$\frac{7}{2}$	$\frac{5}{2}$	...
93	-	$\frac{1}{2}$	$\frac{3}{2}$	$\frac{3}{2}$	$\frac{5}{2}$	$\frac{7}{2}$	$\frac{5}{2}$	...	71	-	$\frac{7}{2}$	$\frac{3}{2}$	$\frac{5}{2}$	$\frac{9}{2}$	$\frac{11}{2}$	$\frac{7}{2}$	...
91	-	$\frac{1}{2}$	$\frac{3}{2}$	$\frac{5}{2}$	$\frac{3}{2}$	$\frac{7}{2}$	$\frac{5}{2}$	...	59	+	$\frac{1}{2}$	$\frac{3}{2}$	$\frac{5}{2}$	$\frac{3}{2}$	$\frac{5}{2}$	$\frac{7}{2}$	...
79	+	$\frac{1}{2}$	$\frac{3}{2}$	$\frac{3}{2}$	$\frac{5}{2}$	$\frac{7}{2}$	$\frac{5}{2}$	...	69	-	$\frac{3}{2}$	$\frac{5}{2}$	$\frac{7}{2}$	$\frac{1}{2}$	$\frac{7}{2}$	$\frac{9}{2}$	...
89	-	$\frac{3}{2}$	$\frac{5}{2}$	$\frac{7}{2}$	$\frac{1}{2}$	$\frac{3}{2}$	$\frac{9}{2}$	...	57	+	$\frac{1}{2}$	$\frac{3}{2}$	$\frac{5}{2}$	$\frac{7}{2}$	$\frac{5}{2}$	$\frac{3}{2}$	...
87	-	$\frac{11}{2}$	$\frac{7}{2}$	$\frac{9}{2}$	$\frac{3}{2}$	$\frac{11}{2}$	$\frac{5}{2}$	...	55	+	$\frac{1}{2}$	$\frac{3}{2}$	$\frac{5}{2}$	$\frac{7}{2}$	$\frac{3}{2}$	$\frac{5}{2}$	...
85	-	$\frac{1}{2}$	$\frac{5}{2}$	$\frac{3}{2}$	$\frac{3}{2}$	$\frac{5}{2}$	$\frac{9}{2}$	...	67	-	$\frac{5}{2}$	$\frac{9}{2}$	$\frac{7}{2}$	$\frac{11}{2}$	$\frac{3}{2}$	$\frac{1}{2}$	...
77	+	$\frac{3}{2}$	$\frac{1}{2}$	$\frac{5}{2}$	$\frac{7}{2}$	$\frac{5}{2}$	$\frac{7}{2}$	...	53	+	$\frac{9}{2}$	$\frac{5}{2}$	$\frac{7}{2}$	$\frac{1}{2}$	$\frac{9}{2}$	$\frac{3}{2}$	...
83	-	$\frac{3}{2}$	$\frac{5}{2}$	$\frac{7}{2}$	$\frac{1}{2}$	$\frac{3}{2}$	$\frac{9}{2}$	...	51	+	$\frac{1}{2}$	$\frac{3}{2}$	$\frac{5}{2}$	$\frac{5}{2}$	$\frac{7}{2}$	$\frac{3}{2}$	...
75	-	$\frac{9}{2}$	$\frac{5}{2}$	$\frac{7}{2}$	$\frac{11}{2}$	$\frac{1}{2}$	$\frac{9}{2}$	...	65	-	$\frac{11}{2}$	$\frac{9}{2}$	$\frac{3}{2}$	$\frac{11}{2}$	$\frac{5}{2}$	$\frac{7}{2}$	...
63	+	$\frac{1}{2}$	$\frac{3}{2}$	$\frac{3}{2}$	$\frac{5}{2}$	$\frac{7}{2}$	$\frac{5}{2}$	...									

(Levels with  $I \leq 11/2$  are listed for the negative parity states,  $I \leq 9/2$  for the positive parity states.)

Since levels of the same parity cannot cross each other, the levels are labeled by the occupation number of the odd nucleon. Since levels of opposite parity do cross each other, however, such a scheme cannot give the order of the single particle levels for all values of  $\beta$ . In Figs. 1. and 2. the particle levels are therefore labeled by the number of the odd nucleon, (Z), for the case of very small deformation,  $\beta$ . Thus, level 81 grows out of the  $s_{\frac{1}{2}}$  shell model state, while levels 79 and 77 grow out of the  $d_{3/2}$  shell model state. For small values of  $\beta$  the wave function for the state 77 becomes predominantly  $\Omega = \frac{1}{2}$  as  $\gamma$  approaches zero. For larger values of  $\beta$ , however, the wave function for state 77 approaches that of a pure  $\Omega = 5/2$  state as  $\gamma$  approaches zero. (Note that the Nilsson levels  $[411] \Omega = \frac{1}{2} +$  and  $[402] \Omega = \frac{5}{2} +$  cross each other at  $\beta \approx .19$ .) The state 77 may therefore be expected to be the state of the odd proton in the isotopes of Re if asymmetric rotator theory is applicable.

Figure 3. shows the rotational energies based on the particle state 77 as a function of  $\gamma$  for relatively small asymmetry and a value of  $\beta$  ( $= .3$ ) which reproduces the experimentally observed value of the electric quadrupole moment for  $\text{Re}^{185}$ . The behavior of these rotational energy levels as a function of  $\gamma$  is characteristic of a large number of particle states. For very small values of  $\gamma$  the particle wave function is predominantly  $\Omega = 5/2$ . The lowest set of rotational states form an  $I = 5/2, 7/2, 9/2, \dots$  sequence with approximate  $I(I + 1)$  spacing. The corresponding wave

functions are almost pure  $K = 5/2$  rotational functions, (corresponding to  $K_R = 0$ ). At  $\gamma = 10^\circ$ , for example, the low  $I = 5/2$  state is 99.98% pure  $K = 5/2$ . The particle wave function, on the other hand, is only 80.7% pure  $\Omega = 5/2$ , with the following admixtures:  $\Omega = \frac{1}{2} : 10.1\%$ ,  $\Omega = -\frac{7}{2} : 7.3\%$ ,  $\Omega = \frac{9}{2} : 1.9\%$ ,  $\Omega = -\frac{3}{2} : 0.1\%$ . The rotational energies of these states first increase with  $\gamma$  since the energies are very sensitive to a small amount of admixture of  $K_R = 2$  near  $\gamma = 0^\circ$  through the  $A_3 \cdot \langle K_R^2 \rangle$  term in the rotational Hamiltonian;  $A_3$  is inversely proportional to  $\sin^2 \gamma$ . In the axially symmetric limit the  $I = 5/2$  ground state has a rotational energy of 0.96 in the units of  $\hbar^2/B\beta^2$  appropriate to Figure 3. A relatively large zero point rotational energy, such as that predicted for  $\gamma \simeq 12^\circ$ , may be important in determining the order of rotational bands based on different particle excitations. For  $\gamma < 11^\circ$  the next set of rotational levels form an  $I = \frac{1}{2}, 3/2, 5/2, \dots$  sequence with  $K_R$  of approximately 2 units. As  $\gamma$  approaches  $0^\circ$  these rotational levels rapidly go to large values through the influence of the  $A_3 \langle K_R^2 \rangle$  term. At  $\gamma = 12^\circ$  the  $I = \frac{1}{2}$  and  $\frac{3}{2}$  levels form the lowest rotational states. At  $\gamma \simeq 12.5^\circ$  the states with  $I \geq 5/2$  have rotational wave functions with almost equal proportions of  $K = 5/2$  and  $K = \frac{1}{2}$ . By  $\gamma \simeq 14^\circ$  to  $15^\circ$  the  $I = \frac{1}{2}, 3/2, 5/2, \dots$  sequence has crossed over the  $I = 5/2, 7/2, 9/2, \dots$  sequence. (Note, however, that levels of the same  $I$  do not actually cross.) The lower sequence now has rotational wave functions of almost pure  $K = \frac{1}{2}$  character while the higher sequence is

predominantly  $K = 5/2$ . At  $14^\circ$  the particle wave function consists of the following admixtures:  $\Omega = 5/2 : 62.6\%$ ,  $\Omega = -7/2 : 21.5\%$ ,  $\Omega = 9/2 : 3.0\%$ ,  $\Omega = \frac{1}{2} : 12.8\%$ ,  $\Omega = -3/2 : .1\%$ . At still larger values of  $\mathcal{H}$  an  $I = 3/2, 5/2, 7/2, \dots$  sequence with  $K_R$  approximately equal to 4 units crosses the  $I = 5/2, 7/2, 9/2, \dots$  sequence and near  $\mathcal{H}$  of  $18^\circ$  the higher levels have strongly mixed  $K = 5/2$  and  $K = -3/2$  rotational wave functions.

The observed levels of  $\text{Re}^{185}$  consist of the following: an  $I = 5/2^+, 7/2^+, 9/2^+$  sequence built on the ground state at 0, 128, and 287 keV; a  $\frac{1}{2}^+, \frac{3}{2}^+$  doublet at 646 and 717 keV; and another  $\frac{1}{2}^+, \frac{3}{2}^+$  doublet at 872 and 879 keV, (with the spin assignment of these last two somewhat uncertain). Mottelson and Nilsson on the basis of the axially symmetric model<sup>9</sup> explain these as the beginning of rotational bands based on the single particle Nilsson levels  $[402] \Omega = \frac{5}{2}^+$ ,  $[400] \Omega = \frac{1}{2}^+$ , and  $[411] \Omega = \frac{1}{2}^+$ , in that order. In terms of the asymmetric model, however, the possibility exists that two of these three rotational sequences are based on the same single particle level (77). With  $\mathcal{H} \simeq 10^\circ$  the spacing of the first five rotational levels corresponds to the observed energies. Since the two apparent rotational sequences at  $10^\circ$  correspond to almost pure  $K = \frac{5}{2}$  and  $K = \frac{1}{2}$  bands even though  $K$  is not a good quantum number in the asymmetric case, it would be difficult to distinguish between an axially symmetric and an asymmetric model. The E2 rates would be very similar in the two cases. Predictions for the magnetic dipole moment differ somewhat since the asymmetric ground state particle wave function is

not a pure  $\Omega = 5/2$  wave function; but these differences are small. The theoretical value on the basis of the asymmetric model is  $\mu = 3.37$  (for  $\beta = .3$ ,  $\gamma = 10^\circ$ ), compared with an experimental value of 3.16 and a theoretical value of 3.7 predicted on the basis of the axially symmetric model<sup>9</sup>. The major differences between the theoretical predictions for the two models would probably involve the transition probabilities between the  $\frac{1}{2}^+$ ,  $\frac{3}{2}^+$  levels and the ground state band. According to the axially symmetric model these transitions would involve a change in the odd nucleon particle excitation. In the asymmetric model, however, transitions from one  $\frac{1}{2}^+$ ,  $\frac{3}{2}^+$  doublet to the ground state would involve no change in the particle wave function. At present there is not sufficient experimental information to decide between the two possibilities. Note that the selection rule  $|\Delta K| \leq 1$  would inhibit the M1 rates between two rotational sequences in the case of both models. Note also that the collective contributions to the E2 rates are small for a  $\Delta K \simeq 2$  transition in the asymmetric model if  $\sin \gamma$  is very small.

The rotational energies in Figure 3. have been drawn only for  $\gamma \leq 18^\circ$ . Near  $\gamma \simeq 20^\circ$  the single particle levels 77 and 63 have very nearly the same energy so that diagonalization of  $(I + \frac{1}{2}) \times (I + \frac{1}{2})$  rotational matrices based on a single particle state cannot be expected to give sensible values for the rotational energies. For  $\gamma > 22.5^\circ$  the difference in energy between the particle states 77 and 63 is again large enough so that the rotational energies can be expected to be

small compared with the difference in particle energies. Now, however, particle state 63, the lower of the two, has a wave function whose character is very similar to that of the state 77 at smaller angles  $\alpha$ . The rotational energies based on particle level 63 should therefore form the natural continuation of the rotational energies of Figure 3. They are shown in Figure 4. for values of  $\alpha$  between  $22.5^\circ$  and  $30^\circ$ . The rotational energies based on particle level 77 for the same range of  $\alpha$  are shown in Figure 5.

Among the isotopes of Ir and Au, which seem to have similar low energy spectra, the experimental situation seems to be most favorable for the isotope  ${}_{77}\text{Ir}^{191}$ . The experimentally observed low-lying states of  $\text{Ir}^{191}$  are shown in the insert of Figure 6. According to the axially symmetric model the low-lying positive parity states might be explained in terms of two rotational bands; the ground state band with  $K = 3/2$  based on the  $[402] \Omega = \frac{3}{2}^+$  Nilsson level, and a nearby band with  $K = \frac{1}{2}$  based on the  $[400] \Omega = \frac{1}{2}^+$  Nilsson level. Because of the proximity of the two states the  $K = \frac{1}{2}$  and  $\frac{3}{2}$  bands would be coupled through the rotation-particle coupling (RPC) term, (Kerman<sup>13</sup>), in the rotational Hamiltonian. According to the asymmetric model, however, the positive parity particle levels 81 and 79 are split relatively far apart even for small asymmetry. (The limiting  $\Omega = \frac{1}{2}^+$  and  $\Omega = \frac{3}{2}^+$  axially symmetric particle levels have very nearly the same energy and are connected by an off-diagonal matrix element when  $\alpha \neq 0^\circ$ .) In the asymmetric model therefore the two

particle states are far enough apart so that the observed rotational states should be based on a single particle state. Figure 6. shows the rotational energies for particle level 79 as a function of  $\gamma$  for the deformation  $\beta = .2$ . Figure 7. shows the rotational energies for the same particle level with  $\beta = .3$ . The low-lying levels have the appearance of two overlapping rotational band systems, one a  $3/2^+$ ,  $5/2^+$ ,  $7/2^+$ , ... sequence, the other a  $1/2^+$ ,  $3/2^+$ ,  $5/2^+$ , ... sequence. (The zero point rotational energies are very large for  $\gamma$  between  $2^\circ$  and  $6^\circ$  since the strong  $\Omega = 1/2, 3/2$  mixing of the particle wave function gives a relatively large  $K_R \simeq 2$  admixture for small values of  $\gamma$  so that the  $\hbar^2 \langle K_R^2 \rangle / 8B\beta^2 \sin^2 \gamma$  term in the rotational Hamiltonian gives a large energy contribution to all rotational levels.) For  $\beta = .2$ ,  $\gamma = 13.50^\circ$ , and for  $\beta = .3$ ,  $\gamma = 9.85^\circ$  the observed levels of  $\text{Ir}^{191}$  are reproduced quite well. For intermediate values of  $\beta$  there is always a value of  $\gamma$  for which the predicted and observed energy spectra are in relatively good agreement.

The theoretically predicted energies are shown in Table III on the basis of both the asymmetric and the symmetric models. In the asymmetric model the rotational constant,  $\hbar^2 / B\beta^2$ , was determined empirically to fit the 129 kev level. The predicted energies for the upper  $5/2^+$  and  $7/2^+$  states are somewhat too high but this is perhaps not disturbing since vibration-rotation interactions have not been taken into account. In the symmetric model the rotational energies were computed by diagonalizing the symmetric rotator



TABLE III

Rotational Energies for Ir<sup>191</sup>

	Experimental	Theoretical Asymmetric Model		Theoretical Symmetric Model with RPC	
		$\beta = .3, \gamma = 9.85^\circ$ <sup>1</sup>	$\beta = .2, \gamma = 13.50^\circ$ <sup>2</sup>	$\beta = .3$ <sup>3</sup>	$\beta = .2$ <sup>4</sup>
$\frac{5}{2} +$	351 Kev	377 Kev	418 Kev	305 Kev	316 Kev
$\frac{7}{2} +$	348	374	415	324	325
$\frac{3}{2} +$	178	173	178	208	206
$\frac{5}{2} +$	129	(129)	(129)	(129)	(129)
$\frac{1}{2} +$	83	87	86	(83)	(83)
$\frac{3}{2} +$	0	0	0	0	0

<sup>1</sup>  $\hbar^2/6B\beta^2 = 29.6$  Kev

<sup>2</sup>  $\hbar^2/6B\beta^2 = 30.8$  Kev

<sup>3</sup>  $\hbar^2/6B\beta^2 = 28.4$  Kev,  $a = .415$ ,  $A = .670$ ,  $\Delta E = 174.5$  Kev

<sup>4</sup>  $\hbar^2/6B\beta^2 = 28.8$  Kev,  $a = .348$ ,  $A = .741$ ,  $\Delta E = 172.5$  Kev

$a$  = computed decoupling parameter,  $A$  = computed RPC parameter,

$$\Delta E = E ( [400] \frac{1}{2} + ) - E ( [402] \frac{3}{2} + )$$

$\hbar^2/6B\beta^2$  and  $\Delta E$  are chosen empirically

Hamiltonian with RPC term. The values of the decoupling parameter  $a$  for the  $\Omega = \frac{1}{2}$  state and the coupling parameter,  $A$ , (Kerman<sup>13</sup>), were computed from Nilsson wave functions and are shown in Table II. In the symmetric case the determination of the rotational energies involved two empirical constants, the energy difference between the  $\Omega = \frac{1}{2}$  and  $\Omega = \frac{3}{2}$  particle states, and a rotational constant,  $\hbar^2/2\mathcal{I} = \hbar^2/6B\beta^2$  which was assumed to have the same value for both bands. Although the predicted energy values may be somewhat better on the basis of asymmetric theory, (if it is borne in mind that vibration-rotation interactions are apt to depress the higher rotational states somewhat), no preference can be given to either model. The rotational wave functions are very similar for both models since the overlapping  $3/2^+$ ,  $5/2^+$ ,  $7/2^+$ , ... and  $1/2^+$ ,  $3/2^+$ ,  $5/2^+$ , ... sequences in the asymmetric model are predominantly  $K = 3/2$  and  $K = 1/2$ , respectively. The ground state which is predominantly  $K = 3/2$  has a  $K = 1/2$  admixture with amplitudes  $C_{1/2}$  between  $-.1$  and  $-.2$  in the case of both models. As a result it is again difficult to distinguish between the two models as far as predicted values of the electromagnetic moments and transition probabilities are concerned. Table IV shows that neither model is very successful in predicting the experimentally observed magnetic moment and in giving consistent predictions for the observed  $M1$  and  $E2$  transition probabilities. (Free nucleon  $g_s$  values

TABLE IV

Electromagnetic Moments and Transition Probabilities for Ir<sup>191</sup>

	Experimental	Theoretical: Asymmetric Model		Theoretical: Symmetric Model with RPC			
		$\beta = .3$	$\gamma = 9.85^\circ$	$\beta = .2$	$\delta = 13.50^\circ$	$\beta = .3$	$\beta = .2$
$\mu$	+ .2 n.m. <sup>a</sup>	-	.42	-	.37	-	.15
Q	$1.5 \pm 1 \times 10^{-24} \text{cm}^2$ <sup>a</sup>	1.47		.93		1.57	1.03
B(M1)	.001 (n.m.) <sup>2b</sup>	.0011		.0009		.0068	.0055
$\frac{1}{2} \rightarrow \frac{3}{2}$ (83 Kev)	.18 <sup>c</sup>	.156		.130		.042	.028
B(E2)	$.10 \times 10^{-48} \text{cm}^4$ <sup>b</sup>	.006		.016		.16	.11
$\frac{1}{2} \rightarrow \frac{3}{2}$ (83 Kev)	.6 ( $\pm .3$ ) <sup>d</sup>	2.15		.92		2.00	.84
$\frac{5}{2} \rightarrow \frac{3}{2}$ (129 Kev)	.4 ( $\pm .1$ ) <sup>e</sup>	.90		.38		.97	.41

<sup>a</sup>W.v.Siemens, Ann. Physik 13, 136 (1953). K.Murakawa and S.Suwa, Phys. Rev. 87, 1048 (1952)<sup>b</sup>A.W.Sunyar, Phys. Rev. 98, 653 (1955)<sup>c</sup>Using a meanlife  $1.4 \times 10^{-10}$  sec. R. L. Mössbauer, Z. Naturforschung 14a, 211 (1959)<sup>d</sup>T.Huus, J.Bjerregaard, B.Elbek, Kgl.Danske Vid. Selsk. Mat.-fys. Medd. 30, No. 17 (1956).  
E. M. Bernstein and H.W.Lewis, Phys. Rev. 105, 1524 (1957)<sup>e</sup>R.H. Davis, A.S.Divatia, D.A.Lind, R.D.Moffat, Phys. Rev. 101, 753 (1956)

are used in all the magnetic moment calculations, and  $g_R$  is set equal to  $Z/A$ . A value of  $R_0 = 1.2 \times 10^{-13}$  cm  $\times A^{1/3}$  is used for all electric quadrupole calculations.) The  $\text{Ir}^{191}$  calculations seem to indicate that it may always be difficult to distinguish between a symmetric and an asymmetric model when the asymmetry is relatively small.

#### ODD N NUCLEI

Figures 8. and 9. show the single particle energy levels for odd N nuclei in the region  $82 < N < 126$  for asymmetries of  $15^\circ$  and  $30^\circ$ , respectively. For the specific deformations  $\beta = .3$  and  $\beta = -.2$  the spin values of the lowest rotational levels based on each particle state are also listed in Table V, (starting with the ground state at the left), in order to give at least some indication of the types of rotational sequences to be expected. Particle levels 121 through 115, and perhaps level 99 may be the pertinent levels for odd parity states of nuclei with A around 190.

The nucleus  ${}_{78}\text{Pt}^{195}$  is of particular interest since its energy spectrum is seemingly fit by asymmetric rotator theory. The experimentally observed energy levels are shown on the left hand side of Figure 10. The levels have been studied through Coulomb excitation<sup>14</sup>, the decay of the metastable  $13/2^+$  level and the positron decay of  $\text{Au}^{195}$  to the low lying states. The most striking feature of the level scheme is that both the upper and lower  $3/2^-$ ,  $5/2^-$  doublets show large electric quadrupole transition probabilities to the ground





Table V (continued)

$\beta = .3 \quad \gamma = 30^\circ$

Order of Low-Lying Rotational Levels for Odd N Nuclei

Particle State	Pa- rity	Spins of Lowest Rotational States Ground State							Particle State	Pa- rity	Spins of Lowest Rotational States Ground State						
125	-	$\frac{1}{2}$	$\frac{3}{2}$	$\frac{5}{2}$	$\frac{3}{2}$	$\frac{5}{2}$	$\frac{7}{2}$	...	97	-	$\frac{1}{2}$	$\frac{3}{2}$	$\frac{5}{2}$	$\frac{3}{2}$	$\frac{5}{2}$	$\frac{7}{2}$	...
123	-	$\frac{1}{2}$	$\frac{3}{2}$	$\frac{3}{2}$	$\frac{5}{2}$	$\frac{5}{2}$	$\frac{7}{2}$	...	109	+	$\frac{9}{2}$	$\frac{5}{2}$	$\frac{7}{2}$	$\frac{11}{2}$	$\frac{13}{2}$	$\frac{1}{2}$	...
121	-	$\frac{3}{2}$	$\frac{1}{2}$	$\frac{3}{2}$	$\frac{5}{2}$	$\frac{7}{2}$	$\frac{9}{2}$	...	95	-	$\frac{3}{2}$	$\frac{1}{2}$	$\frac{5}{2}$	$\frac{3}{2}$	$\frac{7}{2}$	$\frac{9}{2}$	...
135	+	$\frac{3}{2}$	$\frac{1}{2}$	$\frac{5}{2}$	$\frac{7}{2}$	$\frac{5}{2}$	$\frac{3}{2}$	...	107	+	$\frac{7}{2}$	$\frac{3}{2}$	$\frac{5}{2}$	$\frac{9}{2}$	$\frac{11}{2}$	$\frac{7}{2}$	...
133	+	$\frac{13}{2}$	$\frac{9}{2}$	$\frac{11}{2}$	$\frac{5}{2}$	$\frac{13}{2}$	$\frac{7}{2}$	...	93	-	$\frac{1}{2}$	$\frac{3}{2}$	$\frac{5}{2}$	$\frac{3}{2}$	$\frac{7}{2}$	$\frac{5}{2}$	...
119	-	$\frac{1}{2}$	$\frac{3}{2}$	$\frac{5}{2}$	$\frac{3}{2}$	$\frac{5}{2}$	$\frac{7}{2}$	...	91	-	$\frac{1}{2}$	$\frac{3}{2}$	$\frac{5}{2}$	$\frac{3}{2}$	$\frac{7}{2}$	$\frac{5}{2}$	...
131	+	$\frac{5}{2}$	$\frac{1}{2}$	$\frac{3}{2}$	$\frac{7}{2}$	$\frac{9}{2}$	$\frac{5}{2}$	...	105	+	$\frac{5}{2}$	$\frac{9}{2}$	$\frac{7}{2}$	$\frac{1}{2}$	$\frac{5}{2}$	$\frac{9}{2}$	...
129	+	$\frac{1}{2}$	$\frac{3}{2}$	$\frac{3}{2}$	$\frac{5}{2}$	$\frac{7}{2}$	$\frac{5}{2}$	...	89	-	$\frac{3}{2}$	$\frac{5}{2}$	$\frac{1}{2}$	$\frac{3}{2}$	$\frac{7}{2}$	$\frac{9}{2}$	...
127	+	$\frac{11}{2}$	$\frac{7}{2}$	$\frac{13}{2}$	$\frac{9}{2}$	$\frac{3}{2}$	$\frac{11}{2}$	...	103	+	$\frac{11}{2}$	$\frac{7}{2}$	$\frac{9}{2}$	$\frac{13}{2}$	$\frac{3}{2}$	$\frac{5}{2}$	...
117	-	$\frac{1}{2}$	$\frac{3}{2}$	$\frac{3}{2}$	$\frac{5}{2}$	$\frac{7}{2}$	$\frac{5}{2}$	...	87	-	$\frac{11}{2}$	$\frac{9}{2}$	$\frac{3}{2}$	$\frac{11}{2}$	$\frac{5}{2}$	$\frac{7}{2}$	...
115	-	$\frac{1}{2}$	$\frac{3}{2}$	$\frac{5}{2}$	$\frac{7}{2}$	$\frac{5}{2}$	$\frac{3}{2}$	...	85	-	$\frac{1}{2}$	$\frac{3}{2}$	$\frac{5}{2}$	$\frac{3}{2}$	$\frac{5}{2}$	$\frac{7}{2}$	...
113	+	$\frac{1}{2}$	$\frac{3}{2}$	$\frac{5}{2}$	$\frac{5}{2}$	$\frac{3}{2}$	$\frac{7}{2}$	...	83	-	$\frac{9}{2}$	$\frac{5}{2}$	$\frac{7}{2}$	$\frac{11}{2}$	$\frac{9}{2}$	$\frac{3}{2}$	...
111	+	$\frac{3}{2}$	$\frac{7}{2}$	$\frac{5}{2}$	$\frac{1}{2}$	$\frac{7}{2}$	$\frac{9}{2}$	...	101	+	$\frac{13}{2}$	$\frac{9}{2}$	$\frac{11}{2}$	$\frac{5}{2}$	$\frac{13}{2}$	$\frac{7}{2}$	...
99	-	$\frac{1}{2}$	$\frac{5}{2}$	$\frac{3}{2}$	$\frac{5}{2}$	$\frac{3}{2}$	$\frac{7}{2}$	...									

(Levels with  $I \leq 13/2$  are listed for the positive parity states,  $I \leq 11/2$  for the negative parity states.)

state, the E2 strengths being 10 to 30 times the single particle estimates<sup>14</sup>. In a rough way each doublet seems to correspond to a state with a rotational (or vibrational) angular momentum of 2 units. Figure 10. shows that there are actually three different particle energy levels all with theoretically predicted rotational spectra which seem to reproduce the experimentally observed level scheme. All three particle states fall in the region appropriate for the 117<sup>th</sup> neutron in Pt<sup>195</sup>, and all three seem to imply large asymmetry. Moreover for any value of  $\beta$  within the limits to be expected in this region of the periodic table there seems to be a value of  $\gamma$  for which the observed level scheme is reproduced at least tolerably well. For  $\beta = .1$ ,  $\gamma \simeq 30^\circ$ , similarly for  $\beta = .2$ ,  $\gamma \simeq 23^\circ$ , however, particle levels 119 and 121 have nearly the same energy so that rotational energy calculations based on a single particle state may not be valid. For the values of  $\beta$  and  $\gamma$  used in Figure 10. the energy separations between single particle states 119 and 121 seem to be large enough for at least the approximate validity of the simple model. The theoretically predicted  $7/2^-$  and  $9/2^-$  levels which fall above the  $13/2^+$  metastable state are dashed since they would not have been experimentally observed. A  $5/2^-$  state above 259 kev, however, would be in agreement with experiment only if the E2 transition probability from the ground state is small.

The experimentally observed and theoretically predicted values for the magnetic moment are shown in Table VI. These are determined mainly by the particle wave functions since an



TABLE VI  
Magnetic Moment and M1 Transition Probabilities in Pt<sup>195</sup>

	Expt.	STATE 115 $\beta = .1$ $\gamma = 30^\circ$	STATE 121 $\beta = .1$ $\gamma = 20^\circ$	STATE 119 $\beta = .2$ $\gamma = 30^\circ$
$\mu$	.600 n.m.	.689	.726	.667
B(M1)				
$\frac{3}{2} \rightarrow \frac{1}{2}$ (210 Kev)	.047 (n.m.) <sup>2</sup>	.076	.392	.088
$\frac{3}{2} \rightarrow \frac{1}{2}$ (99 Kev)	(.044)	.072	.017	.112
$\frac{5}{2} \rightarrow \frac{3}{2}$ (140 Kev)	.0087	.0056	.242	.014
$\frac{5}{2} \rightarrow \frac{3}{2}$ (31 Kev)	.071	.024	.306	.165

$I = \frac{1}{2}$  level is a pure  $K = \frac{1}{2}$  level for all values of  $\gamma$ . The reduced widths for magnetic dipole transitions seem to rule out the second possibility; but, considering the limitations of the model and perhaps experimental uncertainties, seem to give fair agreement for the other two levels.

The electric quadrupole transition probabilities are shown in Table VII. The asymmetric model fails to predict one of the most striking features of the observed spectrum, the large crossover E2 transition probabilities involving the upper  $3/2^-$ ,  $5/2^-$  doublet. Since this is the most characteristic feature of the spectrum, it must be concluded that the simple asymmetric model does not fit the low-lying levels of  $\text{Pt}^{195}$ . The calculations indicate that a fit of the energy spectrum alone, if only a few states are observed, can never be confirmation of the asymmetric model, since the asymmetric rotator spectrum is very rich in levels which are a sensitive function of  $\gamma$ , so that many different sequences of four or five levels can be reproduced.

Attempts to fit the levels of  $\text{Pt}^{195}$  with a symmetric rotator model seem to indicate only that the nucleus falls into the intermediate coupling region where neither the simple rotational nor the simple vibrational model can be applied. Since the particle states 119 and 121 are nearly degenerate for certain values of  $\beta$  and relatively large  $\gamma$ , the possibility does exist that the observed level scheme can be accounted for in terms of two different particle excitations with rotational wave functions which for the  $I = 3/2^-$ ,  $5/2^-$

Table VII

E2 Transition Probabilities in Pt<sup>195</sup>

B (E2)		STATE 115	STATE 121	STATE 119
$10^{-49} \text{ cm}^4$	Expt.*	$\beta = .1$ $\gamma = 30^\circ$	$\beta = .1$ $\gamma = 20^\circ$	$\beta = .2$ $\gamma = 30^\circ$
$\frac{3}{2} \rightarrow \frac{1}{2}$ (99 Kev)	.90	1.6	1.5	6.5
$\frac{5}{2} \rightarrow \frac{1}{2}$ (130 Kev)	1.0	1.6	1.5	6.5
$\frac{5}{2} \rightarrow \frac{3}{2}$ (31 Kev)		.53	.063	.00005
Cross over $\frac{3}{2} \rightarrow \frac{1}{2}$ (210 Kev)	2.14	.05	.08	.00003
$\frac{5}{2} \rightarrow \frac{1}{2}$ (240 Kev)	1.29	.006	.003	.00003
$\frac{5}{2} \rightarrow \frac{3}{2}$ (140 Kev)	.11	.006	.36	1.84
$\frac{5}{2} \rightarrow \frac{1}{2}$ ( > 259 Kev)		.002	-	.28

\*McGowan and Stelson, Phys. Rev. 116, 154 (1959)

states are strong mixtures of the two states and would therefore give rise to two  $3/2^-$ ,  $5/2^-$  doublets with strong E2 transition probabilities to the ground state. However, much more experimental information would be needed about the nucleus before such a sophisticated interpretation could be adequately tested. It should be noted, however, that no strong E2 cross-over probabilities are observed for the  $2^+$  levels of the neighboring even-even isotopes,  $\text{Pt}^{194}$  and  $\text{Pt}^{196}$ . The assumption that the low-lying levels of  $\text{Pt}^{195}$  involve two different particle excitations may therefore be reasonable.

## REFERENCES

1. A. S. Davydov and G. F. Filippov, J. Exptl. Theoret. Phys. (U.S.S.R.) 35 (8) (303) (1958) and Nuclear Phys. 8, 237 (1958).
2. A. Bohr, Kgl. Danske Videnskab. Selskab. Mat.-fys. Medd. 26 No. 14 (1952);  
A. Bohr and B. R. Mottelson, Kgl. Danske Videnskab. Selskab. Mat.-fys. Medd. 27 No. 16 (1953).
3. C. A. Mallmann and A. K. Kerman, Nuclear Phys. 16, 105 (1960)  
A. S. Davydov and V. S. Rostovsky, Nuclear Phys. 12, 58 (1959)  
R. B. Moore, R. S. Weaver, and W. White, Can. J. Phys. 37, 1036 (1959)  
J. Hiura and S. Suekane, Progr. Theoret. Phys. 24, 462 (1960)  
E. P. Grigoriev and M. P. Avotina, Nuclear Phys. 19, 248 (1960)
4. T. Tamura and T. Udagawa, Nuclear Phys. 16, 460 (1960)
5. T. D. Newton, Can. J. Phys. 38, 700 (1960) and Chalk River Report CRT-886 (1960)
6. S. G. Nilsson, Kgl. Danske Videnskab. Selskab. Mat.-fys. Medd. 29 No. 16 (1955)
7. A. S. Davydov in Proc. of the Int. Conf. on Nuclear Structure. Kingston, Canada. p. 801 (1960)
8. A. S. Davydov, J. Exptl. Theoret. Phys. (U.S.S.R.) 36, (9) 1103 (1959)
9. B. R. Mottelson and S. G. Nilsson, Kgl. Danske Videnskab. Selskab. Mat.-fys. Skrifter, 1, No. 8 (1959)
10. G. Alaga, K. Alder, A. Bohr, and B. Mottelson, Kgl. Danske Videnskab. Selskab. Mat.-fys. Medd. 29 No. 9 (1955)

REFERENCES (continued)

11. K. Helmers, Nuclear Phys. 20, 585 (1960)
12. G. R. Satchler, Ann. Physics 3, 273 (1958)  
A. M. Lane, Rev. Mod. Phys. 32, 519 (1960)  
M. H. McFarlane and J. B. French, Rev. Mod. Phys. 32, 567  
(1960)
13. A. K. Kerman, Kgl. Danske Videnskab. Selskob. Mat.-fys.  
Medd. 30 No. 15 (1956)
14. F. K. McGowan and P. H. Stelson, Phys. Rev. 116, 154 (1959)

Figure 1. Single-Particle Levels for Odd-Z Nuclei in the

Region  $50 < Z < 82$ .  $A = 15^{\circ}$ . The parameters

$C$  ( $\mu$ ) and  $D$  ( $\mu$ ) for these levels have been chosen to have the values recommended by Mottelson and Nilsson, (reference 9). The calculated wave functions correspond to the parameters  $C = - .1$  ( $\mu = .05$ ); and  $D = - .0275$  ( $\mu = .55$ ) for  $N = 4$  (+ parity) levels, while  $D = - .0250$  ( $\mu = .50$ ) for  $N = 5$  (- parity) levels. Since levels of a given parity do not cross, the single particle levels are labelled by their parity and by an ordering number which would be the number of the odd proton if the single-particle levels, at small deformation  $\beta$ , were filled in order. The single-particle levels are also labelled with the spin and parity of the lowest rotational level (ground state) for the specific deformations  $\beta = .3$  and  $\beta = - .2$ .





Figure 2. Single-Particle Levels for Odd-Z Nuclei in the

Region  $50 < Z < 82$ .  $\hbar = 30^0$ . See caption for

Figure 1.



Figure 3. Rotational Energies for the Particle State 77.

$\beta = .3$ . As  $\gamma$  approaches  $0^\circ$ , particle state 77 goes over to the axially symmetric  $[402] \Omega = 5/2^+$  particle state for this deformation.

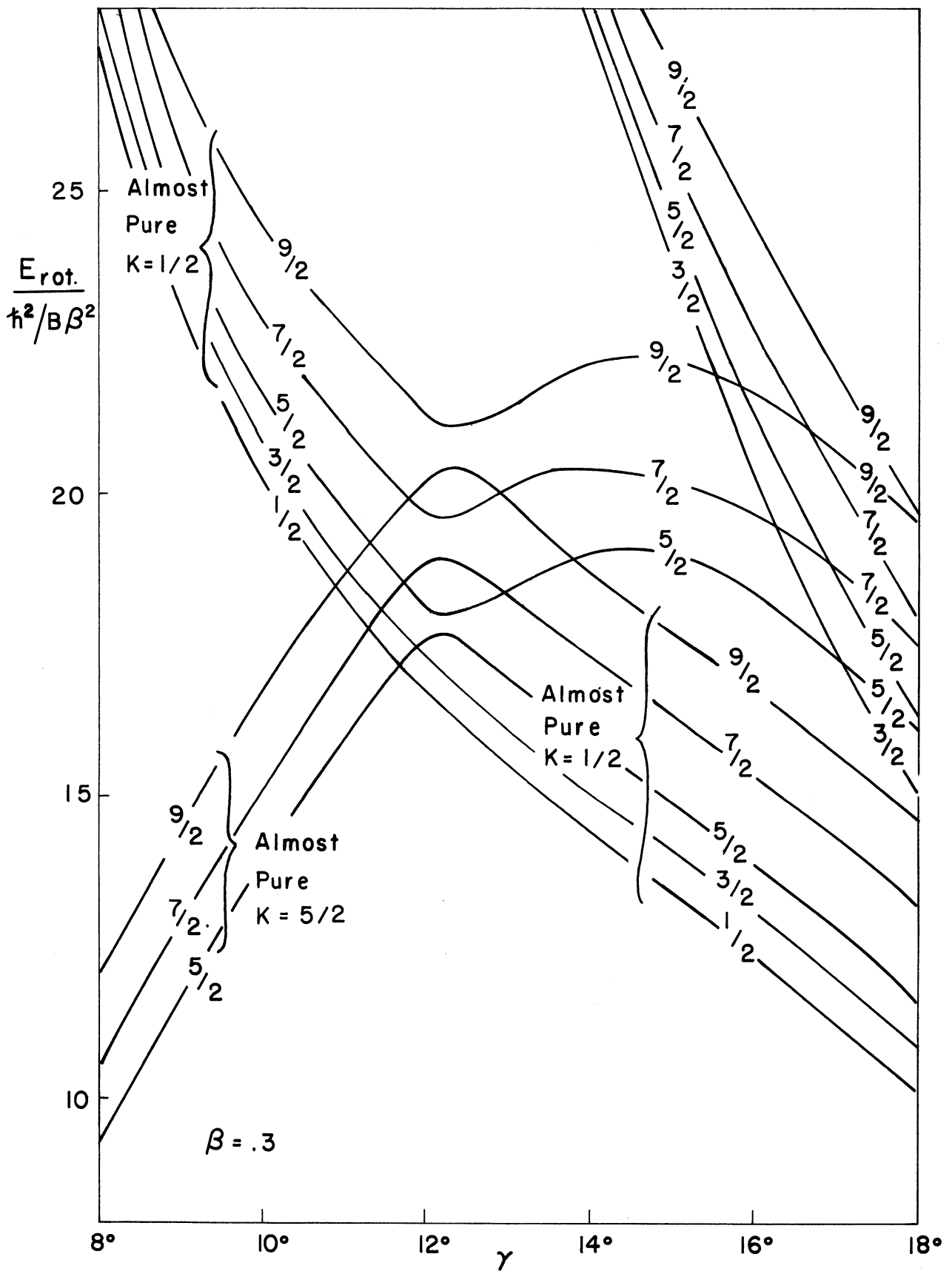


Figure 3

Figure 4. Rotational Energies for the Particle State 63.  
 $\beta = .3$ . ( $\alpha > 22.5^\circ$ ). These are the natural continuation of the rotational levels of Figure 3. Near  $\alpha \approx 20^\circ$  Particle States 63 and 77 are nearly degenerate. For  $\alpha > 22.5^\circ$  the particle wave functions for state 63 are the natural continuation of those for state 77 at smaller angles  $\alpha$ .

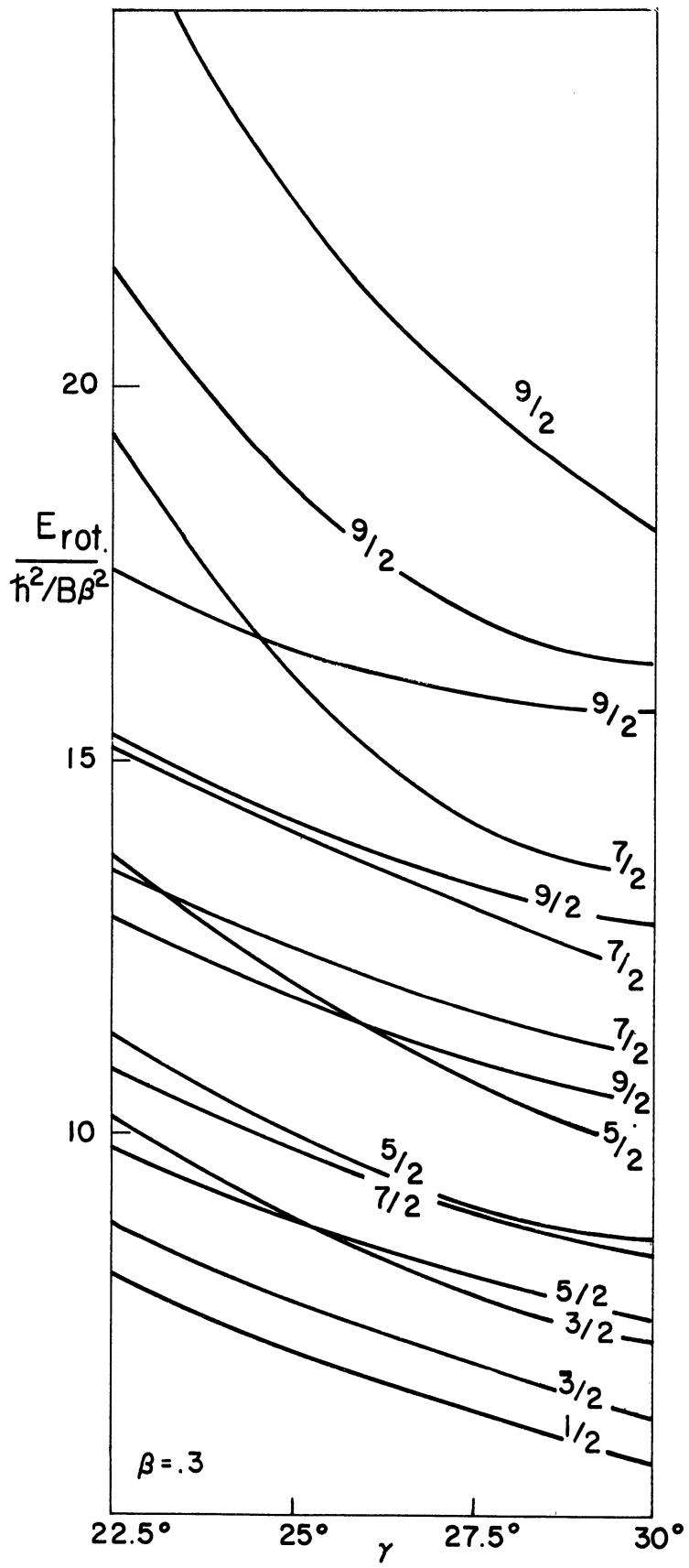


Figure 4

Figure 5. Rotational Energies for the Particle State 77.

$$\beta = .3. \quad (\gamma > 22.5^\circ).$$

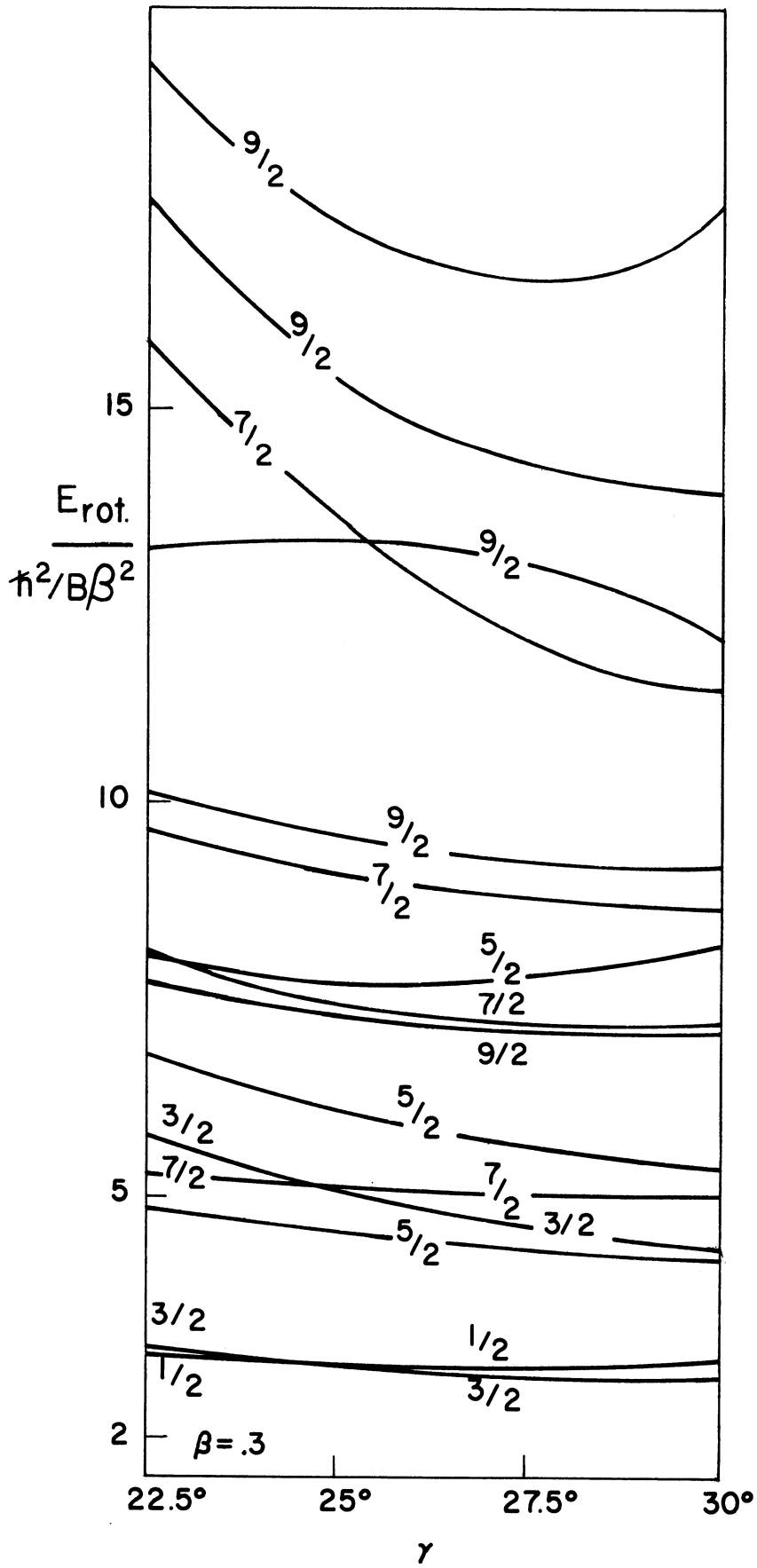


Figure 5



Figure 6. Rotational Energies for the Particle State 79.

$\beta = .2$ . As  $\gamma$  approaches  $0^\circ$ , particle state 79 goes over to the axially symmetric  $[402] \Omega = 3/2^+$  particle state. The insert shows the experimentally observed low-lying energy levels of  ${}_{77}\text{Ir}^{191}$ . Note that the order of the rotational levels for  $\gamma = 13.5^\circ$  ( $\beta = .2$ ) is in agreement with the experimentally observed + parity states in  $\text{Ir}^{191}$ .

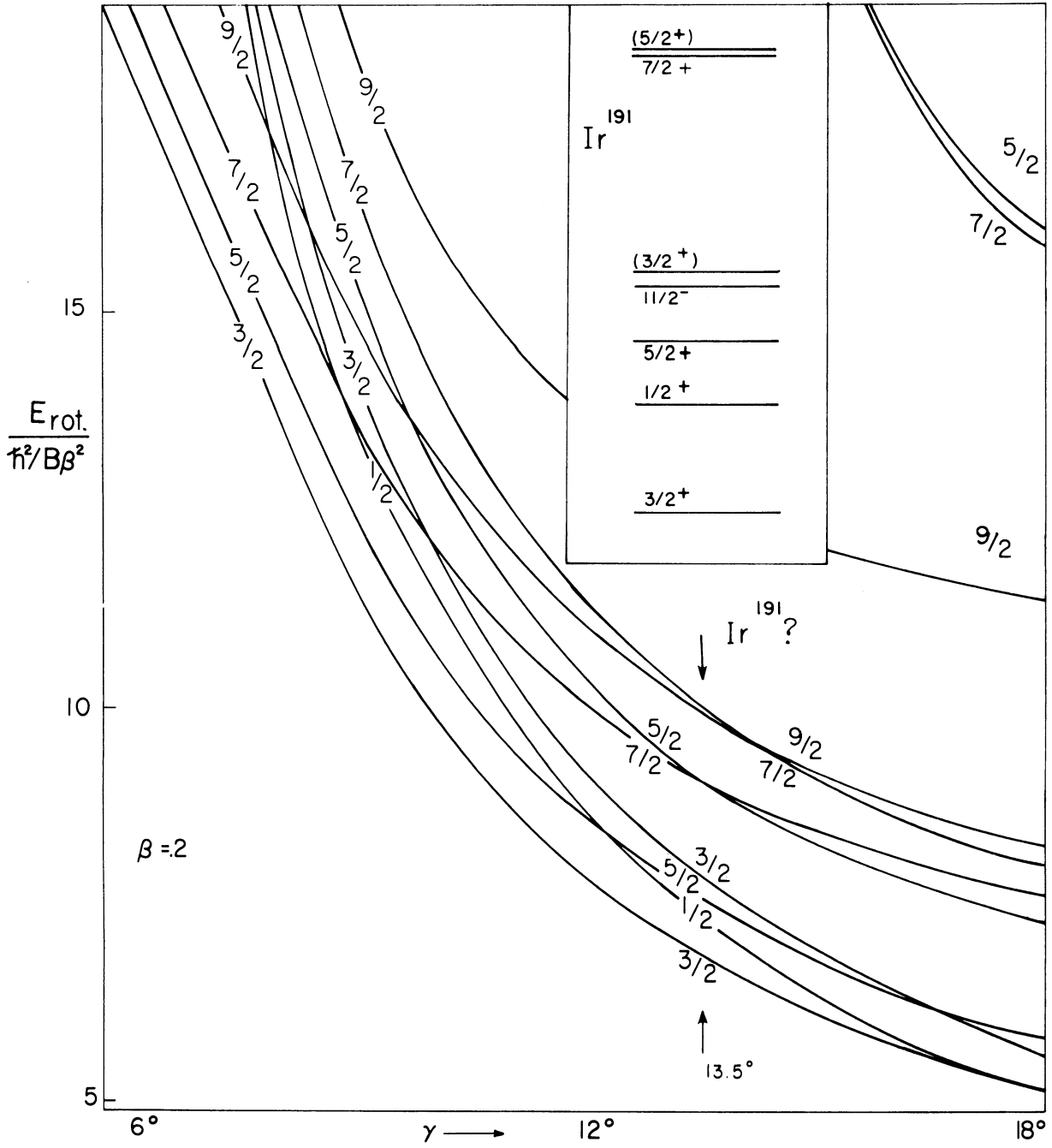


Figure 6

Figure 7. Rotational Energies for the Particle State 79.

$$\beta = .3.$$

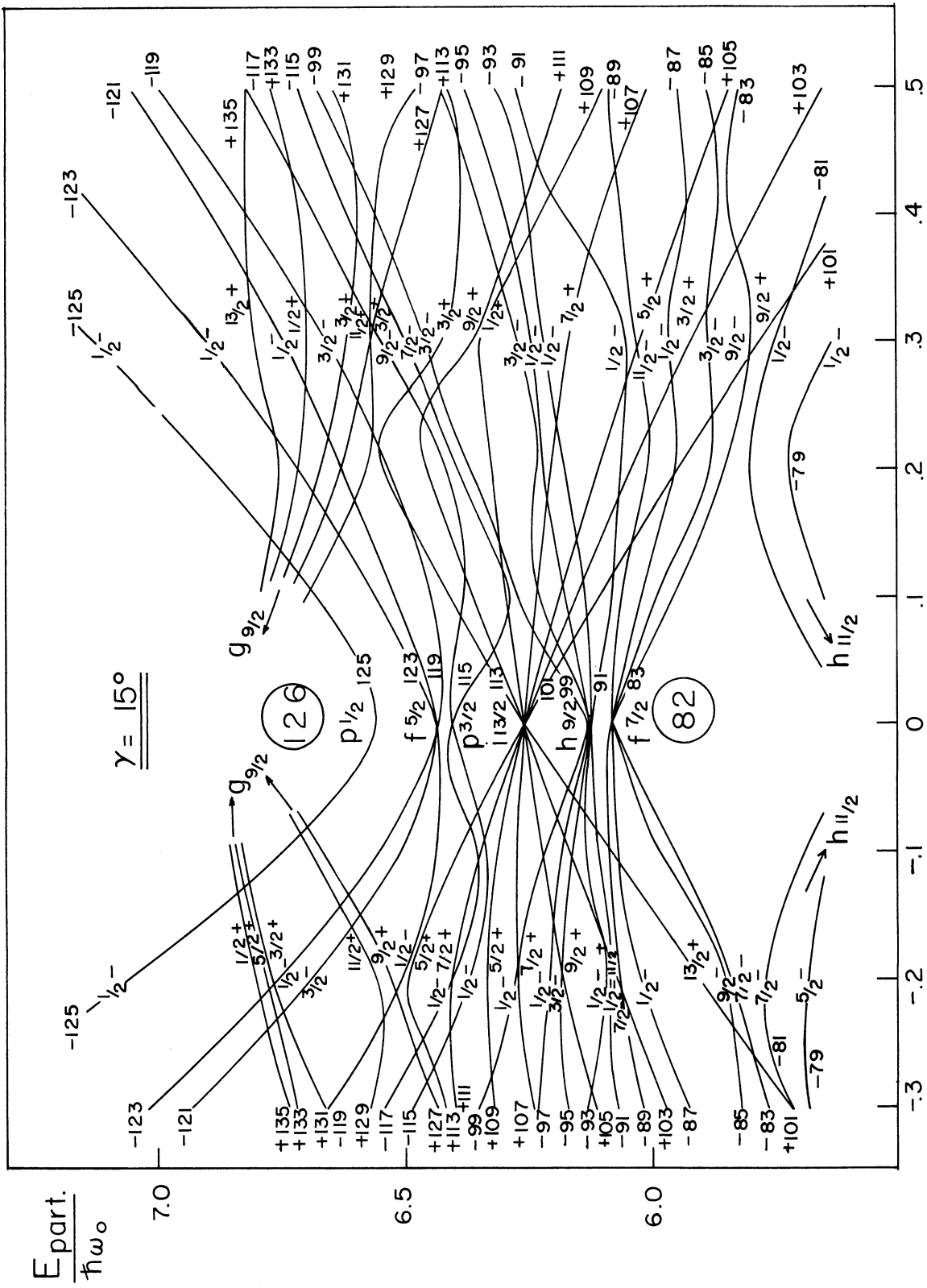


Figure 8. Single-Particle Levels for Odd-N Nuclei in the

Region 82 < N < 126  $\gamma = 15^\circ$ . The parameters

$C(\mathcal{K})$  and  $D(\mu)$  for these levels have been chosen to have the values recommended by Mottelson and Nilsson, (reference9). The calculated wave functions correspond to the parameters  $C = -.1$  ( $\mathcal{K} = .05$ ) and  $D = -.0225$  ( $\mu = .45$ ) for both the - parity  $N = 5$  and + parity  $N = 6$  levels. The levels are labelled by their parity and by an ordering number which would be the number of the odd neutron if the single-particle levels, at small deformation  $\beta$ , were filled in order. The single particle levels are also labelled with the spin and parity of the lowest rotational level (ground state) for the specific deformations

$$\beta = .3 \text{ and } \beta = -.2.$$



$\beta \rightarrow$

Figure 8

Figure 9. Single-Particle Levels for odd-N Nuclei in the

Region  $82 < N < 126$ .  $\chi = 30^\circ$ . See caption for

Figure 8.

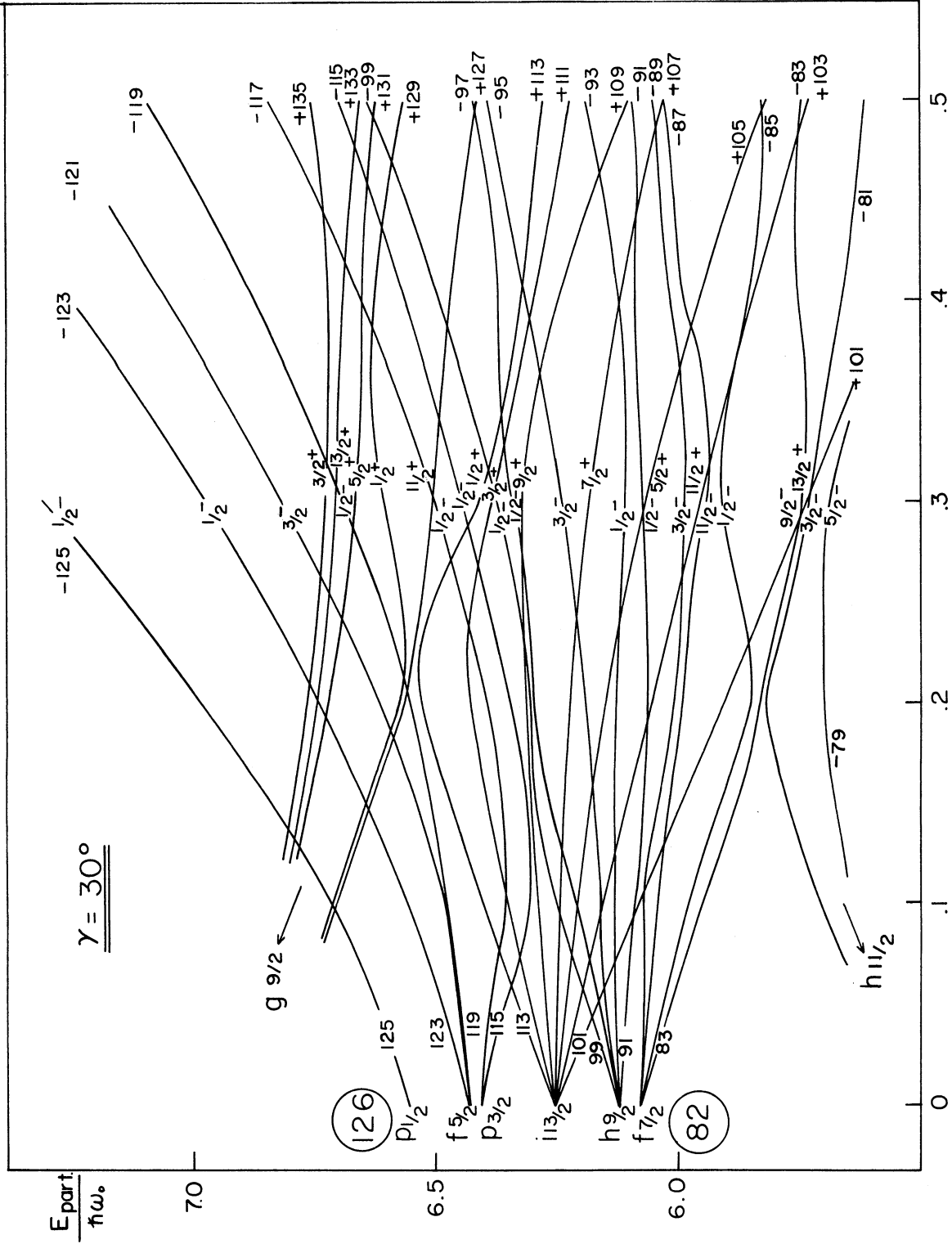


Figure 9



Figure 10. Energy Levels for  ${}_{78}\text{Pt}^{195}$ . The experimentally observed levels are shown on the left. Level schemes predicted on asymmetric rotator theory are shown for three different negative parity particle states in the region appropriate for the 117<sup>th</sup> neutron. Predicted levels with  $I = 7/2$  and  $9/2$  above 250 Kev have been drawn with dashed lines since they would probably not have been experimentally observed. The predicted  $I = 5/2$  levels above 259 Kev are in agreement with the observed facts only if they are connected to the ground state through very small E2 transition probabilities. The rotational constant,  $\hbar^2/B\beta^2$ , has been chosen to fit the 129 Kev level in each case. Values of  $\hbar^2/B\beta^2$  of 80 Kev, 100 Kev, and 82 Kev were used for particle states 115, 121, and 119.

Particle State: 115

121

119

$\beta = .1$

$\beta = .1$

$\beta = .2$

$\gamma = 30^\circ$

$\gamma = 20^\circ$

$\gamma = 30^\circ$

195

Pt

78

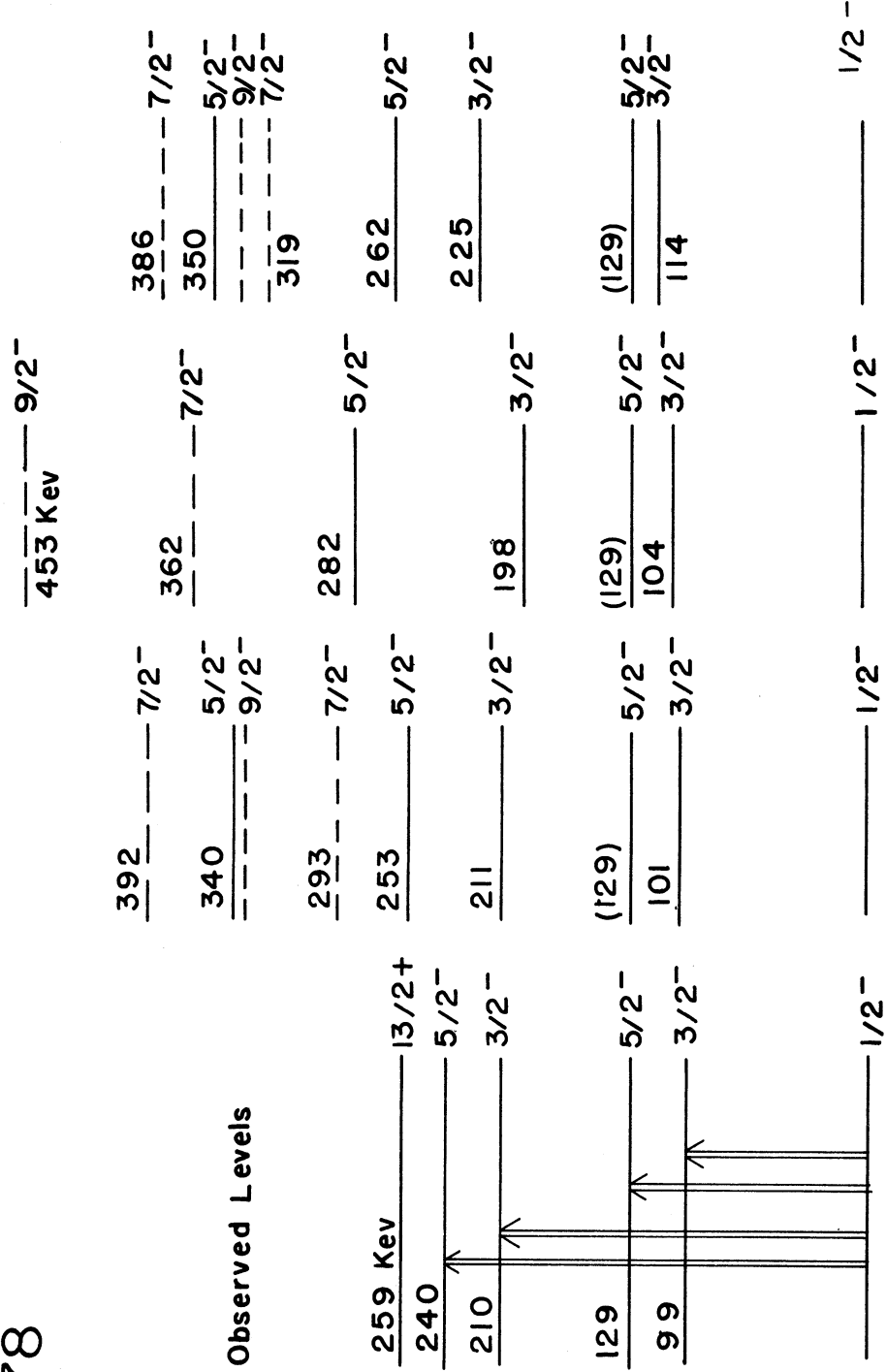


Figure 10





UNIVERSITY OF MICHIGAN



3 9015 03026 6434